Journal of Environmental Management 393 (2025) 126977

Contents lists available at ScienceDirect

Journal of Environmental Management

journal homepage: www.elsevier.com/locate/jenvman

Research article

# Elemental content and radionuclide activity of bottom and fly ashes from Municipal Solid Waste Incineration: a time series analysis

Junaid Ghani [a,b], Katerina Rodiouchkina [c], Ilia Rodushkin [c,d], Enrico Dinelli [a,**], Silvia Giuliani [b], Luca Giorgio Bellucci [b], Thomas Aiglsperger [c], Emma Engström [c,d], Valerio Funari [a,e,*]

[a] University of Bologna, Department of Biological, Geological and Environmental Sciences (BiGeA), Piazza di Porta San Donato, 1, Bologna, Italy
[b] National Research Council of Italy (CNR), Department of Scienze Del Sistema Terra e Tecnologie per l'Ambiente, Marine science institute (ISMAR), Bologna Research Area, via P. Gobetti, 101, Bologna, Italy
[c] Department of Civil, Environmental and Natural Resources Engineering, Division of Geosciences and Environmental Engineering, Luleå University of Technology, 97187, Luleå, Sweden
[d] ALS Scandinavia AB, ALS Laboratory Group, 97775, Luleå, Sweden
[e] National Research Council of Italy (CNR), Department of Scienze Del Sistema Terra e Tecnologie per l'Ambiente, Marine science institute (ISMAR), Napoli Research Area, via Calata Porta di Massa–Porto Di Napoli, 80, 80133, Napoli, Italy

ARTICLE INFO

*Keywords:*
MSWI residues
Characterisation
Element enrichment
Radiological impact

ABSTRACT

Municipal Solid Waste Incineration (MSWI) plants pose significant environmental concerns, generating solid by-products, namely Fly Ash (FA) and Bottom Ash (BA). These MSWI residues have received attention due to the presence of valuable elements, Potentially Toxic Elements (PTE), and other contaminants. Radionuclide detection is also critical because they can concentrate in incineration ashes to pose a radiological hazard. Therefore, multi-element and radionuclide analysis was performed on BA and FA, including samples from bag filters containing lime (FAL) and soda (FAS) additives collected from two MSWI plants in northern Italy. BA and FA were sampled in 2013, 2020, 2021, and 2022 for a multi-year assessment, including during the COVID-19 pandemic. Our objectives were to evaluate the potential of elemental flows and radiological impact of the two different MSWI plants. The chemical concentration of 70 elements and the activity of 8 radionuclides were determined using sector Field Inductively Coupled Plasma Mass Spectrometry (ICP-SFMS) and alpha and gamma spectrometry, respectively. Regarding major elements (Fe, Al, Mg, Ti, and P), high mean concentrations were found in BA, followed by FAL and FAS. Notably, in BA samples, Fe, Al, Zn, and Cu averaged 47600, 35300, 4100, and 3500 mg $kg^{-1}$, respectively, and critical raw materials, namely elements of economic importance such as Mg, P, Ti, and Ba, were concentrated at 16100, 6800, 3500, and 1400 mg $kg^{-1}$, respectively. The annual flows of elements from MSWI residue streams ranged in the order of $10^3$-$10^4$ kg $a^{-1}$ for Fe, Al, Zn, Cu, Mg and Ti, and the sum of Rare Earth Elements (∑REE) was about hundreds of kg per year. Chondrite-normalized patterns of REE and normalized patterns of selected elements over crustal averages helped to evaluate anthropogenic signals, which enabled us to hypothesise elemental sources related to the input MSW. BA and FA showed a higher content of natural radionuclides than artificial ones. In BA, natural radionuclides, $^{40}K$ and $^{210}Pb$, ranged from 666 to 693 Bq $kg^{-1}$ and 23.3–48.1 Bq $kg^{-1}$, respectively. In FA, $^{40}K$ ranged from 308 to 2198 Bq $kg^{-1}$ and $^{210}Pb$ from 17.1 to 534 Bq $kg^{-1}$. Activity concentration index (ACI) results in all-natural radionuclides below the permissible limit (<1). Still, the significant abundance of $^{210}Pb$ and $^{40}K$, coupled with their complex behaviour, calls for new and continuous evaluation of long-term emissions and the radiological hazard related to MSWI systems.

* Corresponding author. National Research Council of Italy (CNR), Department of Scienze Del Sistema Terra e Tecnologie per l'Ambiente, Marine science institute (ISMAR), Napoli Research Area, via Calata Porta di Massa–Porto Di Napoli, 80, 80133, Napoli, Italy
** Corresponding author. University of Bologna, Department of Biological, Geological and Environmental Sciences (BiGeA), Piazza di Porta San Donato, 1 Bologna, Italy
*E-mail addresses:* enrico.dinelli@unibo.it (E. Dinelli), valerio.funari@cnr.it (V. Funari).

https://doi.org/10.1016/j.jenvman.2025.126977
Received 24 February 2025; Received in revised form 30 July 2025; Accepted 12 August 2025
Available online 23 August 2025

## 1. Introduction

Incineration using Waste to Energy (WtE) technology is one of the preferred options for volume reduction and management of Municipal Solid Waste (MSW) in many industrialised countries. Inevitably, two solid byproducts are generated in Municipal Solid Waste Incineration (MSWI) systems. The Fly Ash (FA), which is removed from exhaust flue gases along the Air Pollution Control (APC) system, and Bottom Ash (BA), i.e., the residual material that remains at the bottom of the grate-furnace of the incinerator (Tang et al., 2015), are the two main solid waste "flows" as considered after Brunner and Rechberger (2004). After incineration, approximately 25–30 % of BA and 1–3 % of FA are generated from the original waste input (Jiao et al., 2016). BA is composed of minerals (50–70 %), glass and ceramics (10–30 %), unburned materials (1–5 %), ferrous-metal particles (5–15 %), and non-ferrous-metal particles (1–5 %) (Funari et al., 2024, and reference therein). Typically, FA is composed of fine particles smaller than 200 μm and is classified as hazardous waste in many countries (Quina et al., 2018) due to high concentrations of Potentially Toxic Elements (PTE). On the other hand, BA is usually not included in the list of hazardous wastes (Dou et al., 2017) because BA does not exceed regulatory hazard thresholds, but it still shows a significant level of PTE (Ghani et al., 2023). During the COVID-19 pandemic, incineration and landfilling of medical waste and MSW generated were prioritised over recycling as many waste categories could be infectious (Prata et al., 2020). Production of MSWI residues is increasing with rapid urbanisation. In addition, the pandemic inevitably led to an increase of (micro)plastics in the MSW input, primarily due to the disposal of single-use protective equipment. Substantial quantities of these (micro)plastics are thus processed in MSWI systems because the thermal treatment is believed to facilitate their fragmentation or destruction, despite a general uncertainty related to legislative gaps (Casella et al., 2024) and actual fate (Yang et al., 2021). The strategic importance of such a residue can be high because BA and FA contain valuable elements for urban mining (Funari et al., 2023), including Critical Raw Materials (CRM) for the European Union (European Union, 2020). According to the European Commission (European Commission, 2023), these CRM are a fundamental base for technological development and include elements at high risk of supply, such as Co, Ga, Nb, Li, Rare Earth Elements (REE), and Platinum Group Elements (PGE), amongst other elements, minerals and aggregates.

BA and FA can be considered urban mines because chemical elements can be extracted from their constant production flow (Funari et al., 2015). From this point of view, the chemical characterisation of BA and FA is of paramount importance in a circular economy perspective. BA composition varies among different incinerators, depending on country, seasonality, incinerator technology, and waste collection efficiency (Wang et al., 2019). However, elements in BA and FA generally fall within a relatively narrow range of concentration (Funari, 2022). BA and FA characterisation emphasised their resource recovery potential (Morf et al., 2013; Funari, 2022; Ghani et al., 2023), which may be realised through various traditional and advanced technologies (Funari et al., 2023). As recently reported, CRM present at significant concentrations in MSWI residues can be Co, Ba, V, W, Ga (Valentim et al., 2024), B, Li, Mg, Ti, P, REE, Ag, Au, Os, Pd, and Pt (Funari et al., 2015; Ghani et al., 2023). Resource recovery from MSWI residues can vary across different incinerators and seasons. Time series analysis is crucial to understanding fluctuation in elemental concentrations and identifying controlling factors (e.g., Chuchro et al., 2025). The variation of elemental abundance can uncover dynamics in MSWI process, identifying significant chemical changes that might indicate changes in input MSW and incineration efficiency over time. In addition, the influence of additives, lime and soda, is least explored in existing studies. The two-step process, which involves the addition of neutralising agents, neutralises acid compounds and stabilises volatile elements, making the FA suitable for disposal or beneficial reuse (Dal Pozzo et al., 2016). Therefore, FA at two different steps of the treatment (see section 1.2 in Supplementary Material), FAL (after lime addition) and FAS (after soda addition), would need an assessment, including in time series.

Some radionuclides can concentrate from carbonaceous materials during combustion (Sahu et al., 2014), which can lead to an enrichment of radionuclides such as $^{238}U$, $^{226}Ra$ and $^{210}Pb$ in the residual ash, particularly well-known in FA from coal combustion (Ozden et al., 2018). Coal combustion FA can also contain high concentrations of naturally occurring radionuclides such as polonium ($^{210}Po$), uranium ($^{234}U$, $^{235}U$, $^{238}U$), radium ($^{226}Ra$), and potassium ($^{40}K$) (Janković et al., 2011). Landfilled FA materials eventually showed high levels of radioactivity in their disposal sites (Baxter, 1993). Less is known about the emission of radionuclides from BA due to their coarser and heavier particles, which are reused as aggregates in backfilling, primarily underground, with minimal risk of endangerment to nearby environments. The evaluation of activity and radiological hazard of radon (Rn), uranium (U), thorium (Th) and potassium (K) in BA from coal power plants is relatively well documented (e.g., Mohamed et al., 2023). Therefore, radionuclides in MSWI BA and FA should be quantified more constantly using analytical techniques and statistical models to evaluate radiological hazards and associated health impacts. According to the European Society of Radiology (ESR, 2015), new data on radionuclides can be utilised in the process of monitoring and implementing strategies of the European Basic Safety Standard (2013/59/EURATOM) within the national legislation system.

MSWI ashes can have different elements and radionuclide profiles depending on the incineration facility and combustion conditions. This assessment of radiochemical composition and variability is virtually overlooked in MSWI residues across years and plants. Concurrent analysis of elemental composition and radionuclides is important in material characterisation, with the ultimate goal of achieving the successful and safe recovery of resources from waste for a circular economy. Assessment of time-resolved and multi-plant chemical analysis of BA, FAL, and FAS can provide valuable insights into seasonal variations and assist stakeholders in anticipating future conditions, making informed decisions on responsible resource usage (e.g., Menéndez-García et al., 2024). A knowledge gap exists in the detailed characterisation of BA and FA, especially their radionuclide activity. Filling this gap is necessary for the evaluation of a safe utilisation of BA and FA. Hence, the present study aimed to.

(i) Determine and compare the elemental composition of MSWI samples from two incinerator plants with time series analysis,
(ii) Estimate elemental flows in MSWI residues, and
(iii) Assess elemental concentrations and the activity of radionuclides in BA and FA with enrichment factors and calculations of emission factors.

This study presents the first quantitative estimation of several radionuclides emission from BA and FA related to the single plant and extended to a regional scale.

## 2. Materials and methods

### 2.1. Sampling and pre-treatment

The sampling campaign of FA and BA was conducted in 2013, 2020, 2021, and 2022, from two grate-furnace MSWI plants, located in Ferrara (FE) and Forlì-Cesena (FC) municipalities, Italy (see Supplementary Materials file section 1.1). Thirty samples, including FA samples ($n$ = 19), divided into FAL samples ($n$ = 13) and FAS samples ($n$ = 6), and BA samples ($n$ = 11) were collected (Table 1). In this study, the number of samples is adequate to assess elemental abundances in MSWI residues, considering two MSWI plants, four years of reference data, and three types of MSWI residues to capture potential differences and interrelationships. The sample number represents the diversity of MSWI residues (BA, FAL, and FAS), mainly because the number of samples for

**Table 1**
Descriptions of sample labels, classification of samples, incinerators, and sampling time.

| Sample label | Sample classification | Incinerator | Sampling time | Year |
|---|---|---|---|---|
| 1S | FAL | FE | November | 2013 |
| 2S | BA | FE | November | 2013 |
| 3S | FAL | FC | November | 2013 |
| 4S | BA | FC | November | 2013 |
| 10S | FAL | FE | July | 2020 |
| 11S | FAS | FE | July | 2020 |
| 15S2 | BA | FE | July | 2020 |
| 18S-1 | FAL | FC | July | 2020 |
| 18S-2 | FAL | FC | July | 2020 |
| 19S | FAL | FC | July | 2020 |
| 23S | BA | FC | July | 2020 |
| 26S | FAL | FE | December | 2020 |
| 29S | FAS | FE | December | 2020 |
| 33S | BA | FE | December | 2020 |
| 35S | FAL | FC | December | 2020 |
| 38S | FAL | FC | December | 2020 |
| 41S | BA | FC | December | 2020 |
| 44S | FAL | FE | December | 2020 |
| 45S | FAS | FE | December | 2021 |
| 46S | BA | FE | December | 2021 |
| 47S | FAL | FC | December | 2021 |
| 48S | FAS | FC | December | 2021 |
| 49S | BA | FC | December | 2021 |
| 62S | FAL | FE | December | 2021 |
| 63S | FAS | FE | June | 2022 |
| 64S | BA | FE | June | 2022 |
| 74S | FAL | FC | June | 2022 |
| 75S | FAS | FC | June | 2022 |
| 76S-1 | BA | FC | June | 2022 |
| 76S-2 | BA | FC | June | 2022 |

each category is roughly proportional to the output streams (Table S1) within the two seasons considered (summer and winter). In this proportionality, a higher number of FA samples is required to represent the higher variability of FA compared to BA (Ghani et al., 2023; Funari, 2022).

Lime and soda additives make up a substantial part of the FAL and FAS, respectively. Therefore, elemental concentrations related to the corresponding FA are calculated by subtracting the elemental concentrations determined for the additives. Samples of these additives (Lime and Soda) used at FE and FC were obtained through sampling by the managers of the MSWI plants from their raw material supply, whose origin can be linked to natural rocks from the Balkan areas, according to the disclosure of the same managers. Details on FAL and FAS, including the role of additives are in the Supplementary Materials file section 1.2. Two available types of FA, i.e., lime-doped FA (FAL) and soda-doped FA (FAS), were sampled from "big bags'' following a simple random sampling methodology, while the quenched BA were sampled from outdoor storage sites, following a stratified random sampling methodology, as in Funari et al. (2015). Sampling of MSWI ashes in 2020, 2021, and 2022 was done because they cover the period of COVID-19 pandemic and its aftermath, while the samples from 2013 were used as a pre-pandemic reference. Moreover, the sample of summer 2020 can be considered as the infancy of the potential changes related to the pandemic concerning waste management, including the MSW sent to incinerators. The scheme in Fig. 1 presents the main processing stages, including the MSWI air pollution control (APC) system where FA materials are generated, sampling storage points, and sample and data treatment. Further details of sampling, homogenisation, and pre-treatment are presented in the Supplementary Materials file section 1.3.

### 2.2. Sample preparation

All samples (BA, FAL, FAS, and additives) were prepared for analysis by multi-acid digestion (Fig. 1) with the aid of a hot block (Pontér et al., 2021). Sample manipulation procedures were performed in a clean laboratory (Class 10,000) to reduce as much possible external sources of contamination (Rodushkin et al., 2010). Hydrochloric acid (HCl, 30 %, Sigma-Aldrich Chemie GmbH, Munich, Germany) and hydrogen fluoride (HF, 48 %, Merck, Darmstadt, Germany) used in this study were of ultrapure grade. Nitric acid ($HNO_3$, 69–70 %, Sigma-Aldrich Chemie GmbH, Munich, Germany) was of analytical grade additionally purified

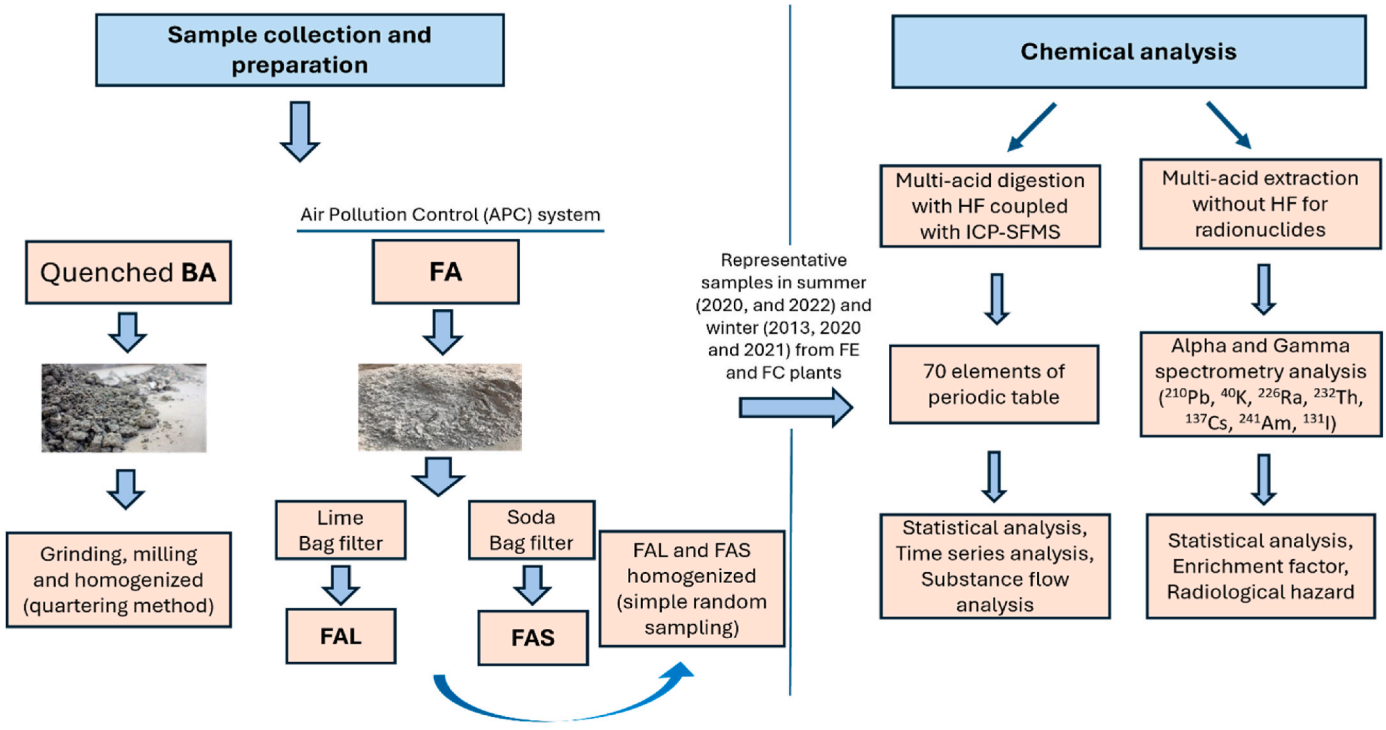


**Fig. 1.** The flow chart of sampling, laboratory activity, and interpretation described in this paper relative to BA and FA from FE and FC MSWI plants. Note: BA; Bottom ash, FA; Fly ash, FAL as Lime-doped fly ash, FAS as Soda-doped fly ash.

in-house by sub boiling distillation. Ultrapure water (Millipore, Bedford, MA, USA) was used for dilution of samples and preparation of blanks and standards.

Homogenised samples (0.5 g) were weighed into 50 ml conical sterile polypropylene centrifuge tubes, one sample for FA and one for BA were weighed in duplicates to evaluate repeatability (18S-1 and 18S-2 for FA; 76S-1 and 76S-2 for BA; Table 1). Exactly 10 ml of HCl and 10 ml of $HNO_3$ were added to all samples and two procedural blanks. Digestion was carried out using a 120 °C hot block under reflux conditions for 24 h. After cooling, 2 ml of HF were added to all tubes and further digestion steps were carried out at 120 °C for a further 2 h. Then, ultrapure water was added up to 50 ml and all tubes were thoroughly mixed. Prior to elemental analysis, samples and blanks were further diluted 100 times in acid-washed (0.78 M $HNO_3$ room temperature leach for 24 h), 12-ml polypropylene tubes with ultrapure water and $HNO_3$ to a total volume of 10 ml and 1.57 M $HNO_3$ matrix. Matrix separation was performed on the remaining sample solution to reduce interferences when measuring trace elements (such as, REE, PGE, and Au), following a modified protocol based on Rodushkin et al. (2018) and Mitra et al. (2021) (Supplementary Materials file 1.3).

### 2.3. Elemental analysis

Elemental concentrations (Ag, Al, As, Au, B, Ba, Be, Bi, Ca, Cd, Ce, Co, Cr, Cs, Cu, Dy, Er, Eu, Fe, Ga, Gd, Ge, Hf, Hg, Ho, I, Ir, K, La, Li, Lu, Mg, Mn, Mo, Na, Nb, Nd, Ni, Os, P, Pb, Pd, Pr, Pt, Rb, Re, Rh, Ru, S, Sb, Sc, Se, Si, Sm, Sn, Sr, Ta, Tb, Te, Th, Ti, Tl, Tm, U, V, W, Y, Yb, Zn, Zr) in ash and additive samples, blanks, and standards were determined using a single-collector double-focusing Inductively Coupled Plasma Sector-Field Mass Spectrometer (ICP-SFMS, ELEMENT XR and ELEMENT 2, Thermo Fisher Scientific, Bremen, Germany). Quantification was achieved by external calibration with synthetic standards and an internal standard, indium (In), was used to correct for potential matrix effects and signal instability (Axelsson et al., 2002; Engström et al., 2004; Rodushkin et al., 2005).

### 2.4. Radiometric measurements

Alpha spectrometry of $^{210}$Po was used for $^{210}$Pb determinations in BA and FA samples from FC, assuming secular equilibrium between the two isotopes, and alpha decays were counted by a silicon surficial barrier detector connected to a multichannel analyzer (Bellucci et al., 2007). Details of the extraction procedure, measurements, software commands for activity calculations, and analytical accuracy are reported in Supplementary Materials 1.4. A selection of samples (representative of each ash category) was analysed based on highest concentrations measured by ICP-SFMS of relevant elements (Pb, Th, and U). The samples considered for comparison were from 2013 to 2022 sampling periods. Natural ($^{210}$Pb, $^{40}$K, $^{226}$Ra, and $^{232}$Th) and artificial radionuclides ($^{137}$Cs, $^{241}$Am, and $^{131}$I) were measured in dry samples using standard vessels of suitable geometries by non-destructive gamma spectrometry (Fig. 1), using Ortec high-purity germanium detectors connected to Ortec DSPEC multi-channel analysers. In gamma spectrometry, $^{210}$Pb was determined from the 46.5 keV peak, $^{242}$Am from the 59.5 keV peak, $^{137}$Cs from the 661.7 keV peak, and $^{40}$K from the 1460.8 keV peak. $^{226}$Ra was determined as a weighted average of the radon progeny, $^{214}$Bi (609.3, 1764.5, and 1120.3 keV peaks), and $^{214}$Pb (351.9, 295.2, and 242 keV peaks). $^{232}$Th was determined as a weighted average of $^{228}$Ac (911.2 and 338.3 keV peaks) and $^{212}$Pb (238.6 keV peak) since these decay products representing $^{228}$Ra and $^{228}$Th were in or close to equilibrium.

### 2.5. Substance flow analysis

Substance flow analysis is a tool used to assess various bio-physical aspects related to human activity across various temporal and spatial scales (Brunner and Rechberger, 2004). In the mass balance calculations, the output materials (BA, FAL, and FAS) derived from (and how much) the input MSW is a well-known information. The flows of output waste for each fraction (BA, FAL, and FAS), in terms of mass per year, are obtained from the annual technical reports of FE and FC MSWI plants, as detailed in the Supplementary Materials (Table S1). Due to the lack of FAS samples suitable for comparison in 2013 and 2020, the mass balance calculation using all fractions (BA, FAL, and FAS) was not possible. Therefore, we used an average of the FAS from other years. Although assuming an average FAS value introduces a source of error, the results of the substance flow analysis can be reliable because the FAS is the smallest fraction in terms of output flows (often less than 1 % of the total waste input). Other necessary assumptions associated to mass conservation principles were: i) the collected BA, FAL, and FAS samples are representative of the entire season/year, ii) the system is effectively closed with no external interferences to the inorganic elements of interest. Details on mass balance calculation are reported in the Supplementary Materials section 1.5.

### 2.6. Assessment of metal enrichment and radiological hazard

Enrichment Factors (EFs) were used to assess the enrichment and behaviour of radionuclides measured in BA and FA for FC plant. The EF was calculated using equation (1) (Ouyang et al., 2018):

$$EF = \frac{(Xs/Ys)}{(Xc/Yc)} \quad (1)$$

Where *Xs* and *Ys* represent the concentration of radionuclides and non-volatile element in BA and FA. *Xc* and *Yc* are the concentration of the radionuclide element and non-volatile element (Ti) in the Upper Continental Crust (UCC; data from Rudnick and Gao, 2014). Titanium is used as a reference element in calculating enrichment factors of BA and FA as Ti is a major constituent of Earth's crust and has chemical stability in solid phases and low volatility during combustion, thus more suitable than other elements (e.g., Cu, Fe, Zr) in the case of MSWI residues.

The Activity Concentration Index (ACI) was used to quantify the radiological hazard of radionuclides, as recommended in the EU Safety Standards (European Commission, 1999). ACI was calculated according to equation (2):

$$ACI = \frac{C_{Th}}{200} + \frac{C_{Ra}}{300} + \frac{C_K}{3000} \quad (2)$$

where $C_{Th}$, $C_{Ra}$, $C_K$ are activity concentrations of $^{232}$Th, $^{226}$Ra, and $^{40}$K, respectively, expressed in Bq kg$^{-1}$.

The Total Emission Factor (TEF) was used to calculate average annual radionuclides activity at the provincial level, using a standard emission factor-based approach (Sahu et al., 2017). The TEF was calculated, using (3):

$$E_x = \Sigma\ (F\ X\ N)\ X\ SMR \quad (3)$$

where *Ex* is the total emission of radioactivity (in Bq); *F* represents the quantity (in kg) of BA and FA generated annually for each incinerator; *N* is the total number of incinerators, while *SMR* is the sum of all measured radioactivity (in Bq kg$^{-1}$) in BA and FA. Further details of EF, ACI and TEF are in the Supplementary Material section 1.6.

## 3. Results and discussion

### 3.1. Chemical composition of BA, FAL, and FAS

The elemental composition of BA and FA (FAL, FAS) samples from FE and FC are presented in Fig. 2. Table S2 and Table S3 of the Supplementary material file report descriptive statistics (minimum, maximum, median, mean and standard deviation) and the complete results of measurements by ICP-SFMS, respectively. BA has, in general, the highest concentration of most elements except volatile elements, followed by

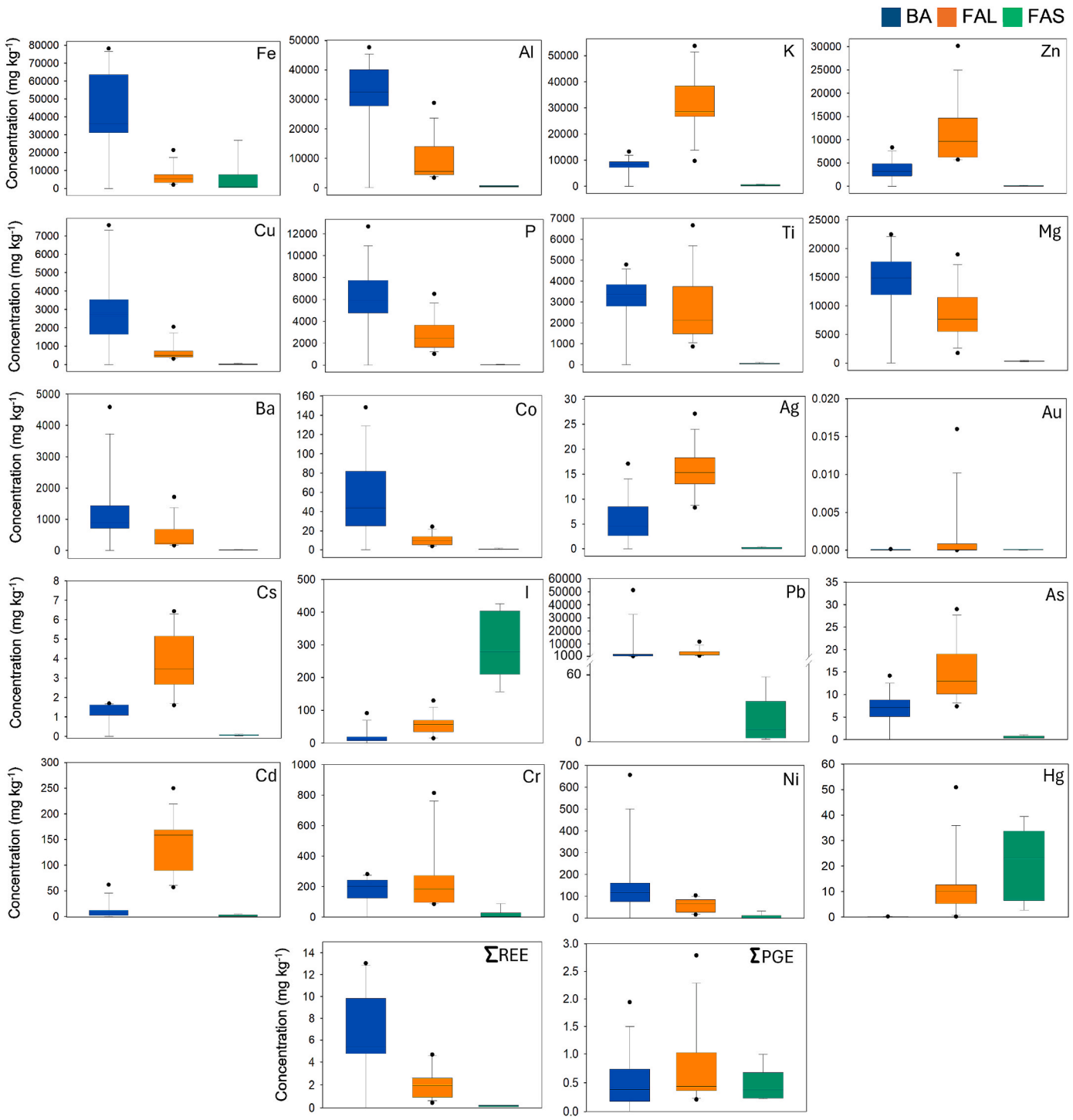


**Fig. 2.** Box plots of selected valuable elements in BA, FAL, and FAS. Industrial base metals (Fe, Al, K, Zn, and Cu); CRM (P, Ti, Mg, Ba, Co, REE, and PGE), precious elements, Ag and Au, and PTE (As, Br, Cd, Cr, Cs, Hg, Ni, and Pb). PGE expressed in μg $kg^{-1}$. ∑REE: La, Ce, Pr, Nd, Sm, Eu, Gd, Tb, Dy, Ho, Er, Tm, Yb, and Lu; ∑PGE: Ru, Rh, Pd, Os, Ir, Pt.

FAL and, lastly, FAS. This concentration difference is expected as: 1) BA consists of all waste products and non-volatile materials that combust completely or partially during the MSWI process, resulting in high elemental concentrations, and 2) elemental concentrations in BA are not diluted by the alkaline additives in contrast to FAL and FAS. Since FAL derives from the first step in cleaning the flue gases, it can scrub a higher particle-leaded stream compared to the second step of the clean-up process, i.e., FAS, along the APC line. Only highly volatile elements, or those that are more stabilised by soda than by lime, will remain in higher concentrations in the FAS category. For example, K, Zn, Pb, As, Cr, and Cd tend to follow this pattern. In Table S2, the average concentration of all elements in BA and FA (FAL, FAS) are compared to UCC average values (from Rudnick and Gao, 2014) to assess their potential in elemental resources.

### 3.1.1. *Industrial base metals and other valuable elements*

Calcium and Na are the most abundant elements in all sample categories; BA and FAL show high Ca concentrations of 189 g $kg^{-1}$ and 197

g $kg^{-1}$, respectively, and FAS shows high Na concentrations averaging 306 g $kg^{-1}$ (Table S3). FAL and FAS are enriched in Ca and Na due to the addition of calcium hydroxide $(CaOH)_2$ and sodium bicarbonate ($NaHCO_3$), respectively. In BA and FA, concentrations of base elements (K, Zn, Cu, Fe, and Al, but Cu, in FAS) are higher than their respective UCC averages (Table S2). Fig. 2 shows how Fe and Al vary in all samples. Both Al and Fe reach maximum concentration in BA, followed by FAL and FAS. The abundance of these elements in BA can be associated with metallic scraps and mineral phases that are not volatilized during combustion (Bunge, 2015). Potassium and Zn reach maximum concentration in the FAL category, followed by BA and FAS (Fig. 2). Although K and Zn occur as major constituents in minerals found in BA (Funari et al., 2024), their volatile part can condense in chlorides as temperature drops in the APC system, and accumulate in FA, also influenced by the organic matter contents (Rissler et al., 2020). K and Al concentrations are comparably low in Chinese MSWI FA (Han et al., 2021). Copper is more concentrated in BA than FAL and FAS, likely forming stable mineral phases (Nguyen et al., 2024). Fe and Cu can be found at high concentrations in BA (Yao et al., 2010), and our results, especially for Zn and Cu, are similar to those of Zhao et al. (2021). Regarding FAL, Zn and Cu concentrations can be higher in Chinese FA containing a lime additive (Lou et al., 2023).

### 3.1.2. Critical Raw Materials (CRM)

In Fig. 2 and Table S2, chemical concentrations of CRM for both FE and FC plants and in all sample categories (BA, FAL, and FAS) are provided. CRM concentrations are one order of magnitude higher than the UCC averages, except Ba that is 30 times lower in FAS and slightly lower in FAL than the UCC. In BA, Mg Ti, P, and Ba show highest concentrations due to their non-volatile nature. In BA, Mg can be present at high concentrations due to the accumulation of Mg-oxides, which tend to remain in the solid residual phase during combustion (e.g., Smołka--Danielowska et al., 2019). BA and FAL show comparable Ti concentrations, and high Ti in FAL is likely due to external contamination from the scrubbing process, such as, the corrosion of exchanger tubing (Kermani et al., 2007). Phosphorus is generally higher in BA than FA. In BA, Mg and Ti contents are higher than those from Japan (Back and Sakanakura, 2021) and other MSWI plants in the USA, UK and Denmark (Gökelma et al., 2021). The formation of stable minerals from organic waste can explain high P contents (Kasina et al., 2023). Barium is typically retained in BA instead of being volatilized, due to its high boiling point (Frandsen et al., 2004).

In FA, CRM, such as, Sr, B, Li, V, Co, W, Nb, Ga, Hf, and Be are mainly concentrated in FAL, followed by FAS (Tables 2 and 3). The alkaline nature of the additives may influence major mineral's formation in FA and final concentration of these valuable elements. CRM concentrations measured for FC and FE plants align to data of FA from EU countries (Nedkvitne et al., 2021). In BA, CRM, such as, Mg, P, Ti, Ba, Sr, B, Li, V, Co, W, Nb, Ga, Hf, and Be are likely hosted in carbonates (Xiang et al., 2022), spinels, metallic inclusions (Funari et al., 2018), melilites, hercynites, non-silicate minerals, and other glassy phases (Mantovani et al., 2023). These minerals are difficult to destroy and can contain inclusions of volatile elements that are not released during incineration, resulting in the relative enrichment of naturally incompatible elements in BA materials (Funari et al., 2024). In the following order, MSWI-BA, FAL, and FAS, can source CRM. A few CRM, including Sb, Bi, and W, are remarkably enriched compared to the Earth's crust (Table S2). Knowing the concentration differences between these materials can be useful to improve CRM extraction from MSWI residues.

### 3.1.3. Rare Earth Elements (REE)

The observed variability of REE concentrations is in Fig. 2. Generally, REE abundance is higher in BA compared to other categories (Fig. 2), likely due to high REE boiling point (Zhao et al., 2008). In BA, the sum of Light REE (ΣLREE) ranged 52.3–236 mg $kg^{-1}$, while the sum of Heavy REE (ΣHREEs) ranged 12.4–25.4 mg $kg^{-1}$. Their concentrations are ten times higher in BA than FAL (ΣLREE 5.12–62.4 mg $kg^{-1}$ and ΣHREE 1.7–26.4 mg $kg^{-1}$), and even much higher than FAS (ΣLREEs 1.2–2.83 mg $kg^{-1}$, ΣHREEs 0.3–0.7 mg $kg^{-1}$).

Ce is generally the most abundant REE in BA (Table S2). The presence of Ce in MSWI residues may be related to its use in glass, cast iron, and stainless steel production (Zambon et al., 2021), which ultimately ends up as MSW (inadequate collection of C&D, Construction and Demolition Waste streams, for instance). REE such as La, Gd, Dy, and Ho are also concentrated in BA. The enrichment of these elements can be attributed to their use in various industrial applications. Lanthanum, for example, is commonly used in battery alloys, laptops, cell phones, hybrid vehicles, and as a glass additive (Perry and Van Veen, 2024). Gadolinium finds applications in products like microwaves, optical components, compact discs, TV tubes, and alloys (Rogowska et al., 2018). The HREE, Dy, is used in permanent magnets (King and Eggert, 2022), Ho in glass polishing and glass additives (Kolawole et al., 2021). Notably, unsorted WEEE, Waste from Electrical and Electronic Equipment, can contribute most to HREE presence in feedstock of incinerators. At the end of their life cycle, all these goods and products can contribute to enhancing REE concentrations in MSWI residues.

The solubility and chemical behaviour of REE can be influenced by the presence of salts, especially Soda and Lime additives in MSWI FA. In general, chlorides and carbonates chemically interact with REE, forming insoluble phases and influencing the partitioning and behaviour of REE. However, the raw material (Lime and Soda additives) used in the APC system leading to FA generation shows uneven chondrite-normalized patterns of about one order of magnitude lower than FAL and FAS values, respectively (Fig. 3), so additives in FA should not superimpose the signals from MSW. In Fig. 3, chondrite normalisation helps to understand the geochemical behaviour of REE in BA and FA. The REE chondrite-normalized patterns of BA show consistency, considering the prolonged observation (Fig. 3). In BA, fluctuation appears for Ce in Dec-2020 samples and Ce, Pr, Nd, Gd, and Ho in 2022 ones. In general, the BA trend adheres to UCC chondrite-normalized patterns. Conversely, the FA patterns slightly differ from UCC chondrite-normalized patterns showing uneven abundances between LREE and HREE. Anomalous behaviour (Ce, Nd, and Yb in FAL; Nd, Gd, and Yb in FAS) may be partly related to the composition of additives (Fig. 3). In FAL, REE patterns show similarity between the yearly samples, but anomalies are visible for Ce, Tb, and Yb in 2013 and Dec-2020 samples. The FAS chondrite-normalized patterns have Gd and Ho peaks in Dec-2020 samples. According to Fig. 3, the relative abundance of LREE such as Ce, Tb, Nd, and Gd is high in BA and FAL, while HREE shows low enrichments. However, HREE partitioning compared to the UCC chondrite-normalized patterns might reflect that REE are often encapsulated in aluminosilicates and other glassy phases, which are typically found in MSWI BA and FA.

### 3.1.4. Potentially Toxic Elements (PTE)

In BA and FA, PTE concentrations are different to the UCC averages. For example, Cr, Cd, As, Ni, and Hg are high in BA and FAL, particularly in BA, and less concentrated in FAS, with some exceptions (Hg; Fig. 2; Table S2). Ni and U are comparably higher in BA samples; Cd, As, and Tl in FAL, and Hg in FAS. Significant concentrations of Cr, Mo, and Pb can be found in BA and FAL. At elevated temperatures, Pb tends to occur as oxides (Świetlik et al., 2016), contributing to Pb enrichment in BA and FA. In FAL, high concentrations of As, Cr, Cd, Hg, and Ni can also be due to their ability to volatilise (>500 °C) and condense in the FA residue (Lu et al., 2022). Thereby, PTE tend to condense in the cooler areas of the APC system where FA is collected (Frandsen et al., 2004). The different speciation of PTE, like Pb, Cr, As, and Cd, can affect their behaviour in the residual ashes (Yao et al., 2017).

Table S4 reports a brief literature analysis regarding most common PTE in MSWI residues. Chemical concentrations of Pb, As, and Cr are similar to reported values from grain-sized BA of the same MSWI plants (Mantovani et al., 2023; Ghani et al., 2023) and other samples of BA and FA from MSWI plants of the same Italian region, collected in 2015

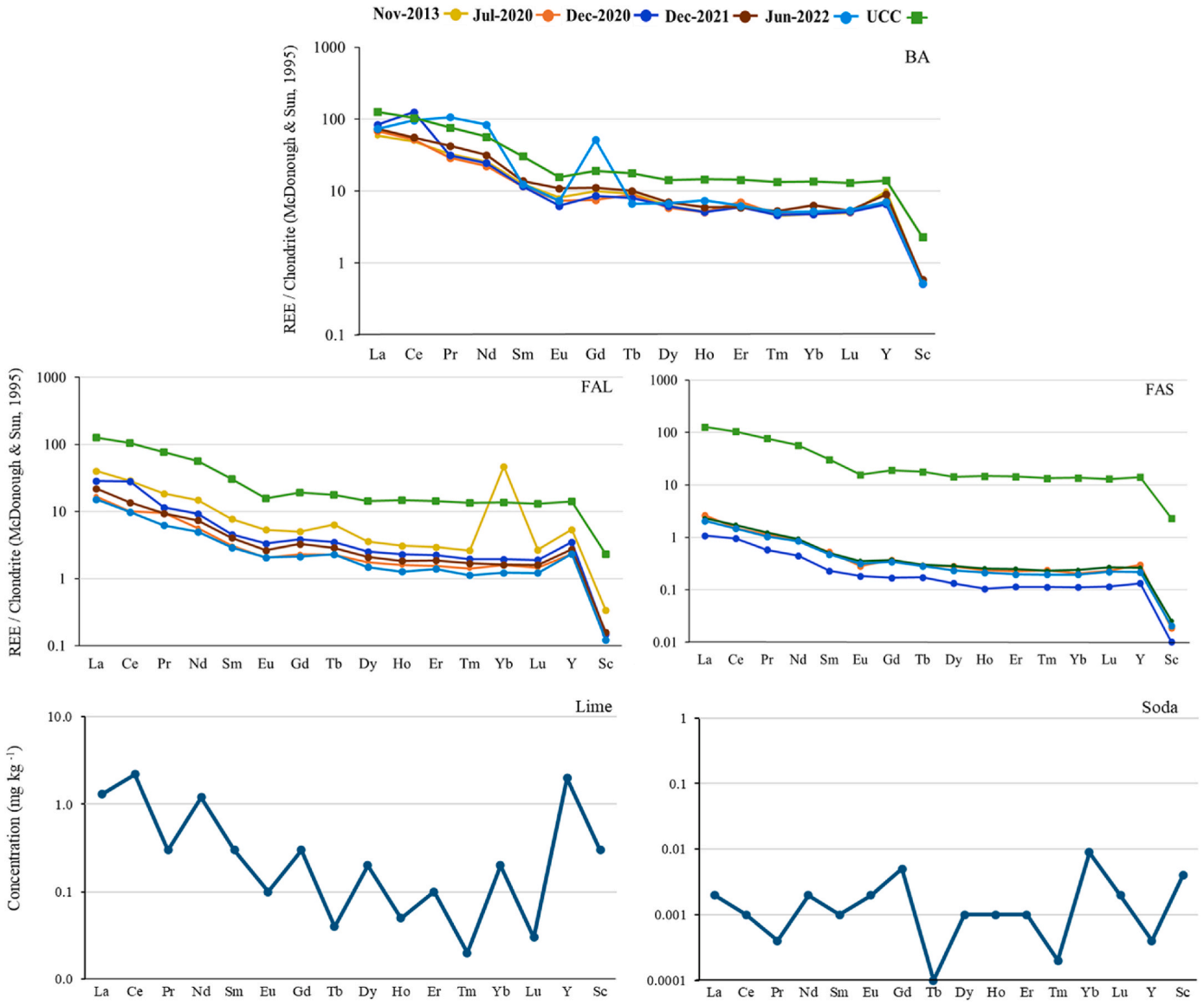


**Fig. 3.** Chondrite-normalized REE in BA, FAL, and FAS samples from 2013 to 2022, based on the carbonaceous chondrite averages by McDonough and Sun (1995). Lime and Soda samples normalized values are also reported to appraise the contribution onto FAL and FAS, respectively.

(Funari et al., 2015) and 2016 (Funari et al., 2016a). In BA, Pb and Cd concentration data are higher than those from Qatar (Al-Ejji et al., 2023), whereas, in FA, the mean concentration of several PTE (Cr, Pb, As) is lower than that reported from MSWI plants in Switzerland (Weibel et al., 2018) and China (Lujiashan plant in Beijing; Zhao et al., 2021).

### 3.1.5. *Platinum Group Elements (PGE), Au, Ag, Re, Sn, Zr, Th, Br, and I*

PGE are Pd, Ru, Pt, Rh, Os, and Ir, listed as "critical raw materials" due to their strategic importance in the EU economy. Like REE, PGE are extensively used in modern industrial applications. The main source of PGE in incinerator ashes is linked to advanced electronics, jewellery, and special alloys wastes (Romano et al., 2023). PGE are at low concentrations in MSWI residues (Fig. 2 and Table S2). PGE concentrations show selective enhancement among the different sample types. BA and FA, especially FAL, show significant Pd and Ru concentrations compared to the UCC average. Ru is higher in BA or FAL than the UCC average (Table S2). As previously reported (Funari et al., 2016b), Os is higher in FAS, and significantly higher than UCC average. Other PGE, Pt, Rh, and Ir, can vary within very low concentrations with differences attributable to their volatility (e.g., Ajorloo et al., 2022).

Similarly, Au, Ag, Re, and Sn, typically present at significant concentrations in FAL samples, can be associated to WEEE, catalysts, jewellery, and special alloys (e.g., cans as a major Sn source; Wei et al., 2011). Th and Zr show high concentrations in BA, likely associated to refractory materials (glass, ceramics) from C&D, WEEE, and other special waste streams (e.g., Lemaignan, 2012; Keith et al., 2019; Ebert et al., 2020). Halogens, like Br and I, are higher in FA due to their volatility (Ebert, 2021). The highest mean concentrations are measured in FAS samples (Table S2). Regarding the potential sources of Br and I, Br is related to flame-retardants, textiles, and plastics, while I mostly to medical waste (Vainikka and Hupa, 2012; Witard et al., 2022).

## 3.2. *Time series analysis of elemental abundance*

A time series of chemical analysis helps to understand patterns of seasonal variation for a given product, which in turn informs policy-making. In the assessment of MSWI residues, time series analysis can be a powerful tool for understanding changes in waste composition over time, reflecting shifts in population habits or sorting practices. The COVID-19 pandemic ineluctably changed the waste management

scenario worldwide. In Italy, incineration was extended to its full capacity. Time series analysis of BA, FAL, and FAS for two plants (FE and FC) spans from 2013 to 2022, with a gap from 2014 to 2019 (Fig. 4).

In BA, FAL, and FAS, most elements show a decrease in concentrations with time, probably because of continuous phasing out of hazardous products and a more efficient waste recycling strategy. Elemental concentrations of BA samples in FC and FE plants are similar (Fig. 4). These results suggest that BA from these plants are more homogenous than FA, where fluctuation in volatile element concentrations can be found (BA: Fig. S1 and Fig. S4 vs FA: Fig. S2, 3 and 5 and Fig. S6). In BA, the concentration of Fe, Cu, Ba, Ti, Cr, and As tends to decrease with time (Fig. 4), although some peaks are randomly observed (Co, W, Pb, Cd, Ni, and PGE; Fig. S4). Conversely, K, P, and Mg concentrations globally increase in both plants. The precious elements Ag and Au are

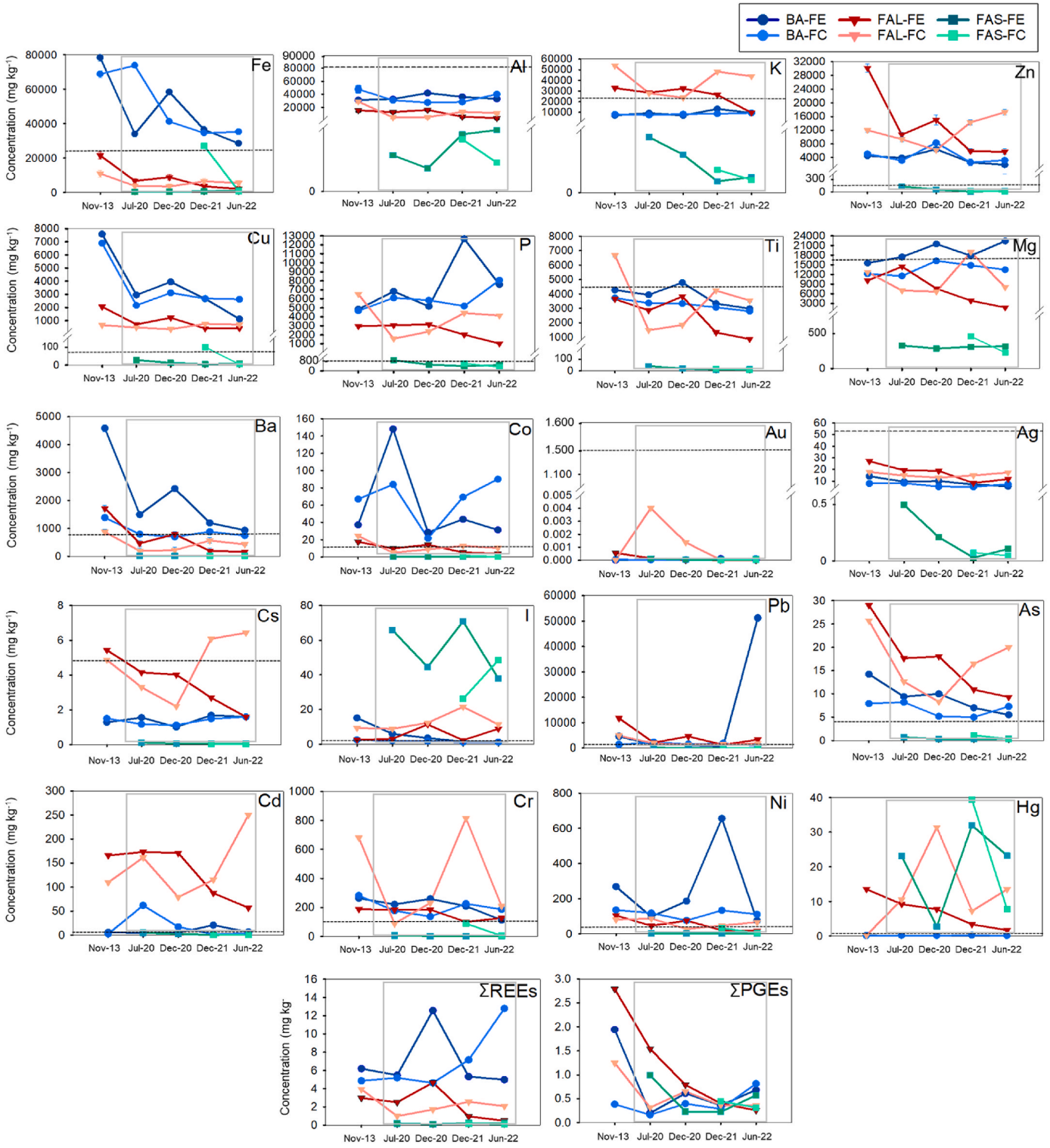


**Fig. 4.** Mean concentrations (mg $kg^{-1}$) of selected elements in BA, FAL and FAS from FE and FC plants. The dotted line represents UCC average values. Refer to Fig. 2 for the element selection. The squared area within each plot highlights the pandemic period.

chemically stable and typically concentrate into BA more than FA (Fig. 4). Au more than Ag can partition in BA, consistent with earlier observation (e.g., Wielinski et al., 2021).

The FAL category shows different patterns among years and MSWI plants (Fig. S5). However, a generalised decrease is observed in the FE plant. In particular, Fe, Cu, Zn, Ba, Ag, PGE, Pb, and As abruptly decreased compared to 2013-sample data (Fig. 4). The FC plant shows a generalised increase of P, Mg and Cs concentrations, peaking in Dec-21 and Jun-22 samples. The FAS category was missing an FC plant's sampling in 2013 and 2020; however, observations can be made, focusing on the FE plant. The concentrations of several elements (K, Zn, P, Ti, Ag, Pb, Cd, and PGE) decrease, especially from 2020 to 2022 (Fig. 4; Fig. S6). Aluminium is the only element that consistently increased with time in the FAS samples of the FE plant (Fig. 4; Fig. S3). In the shorter record of the FC plant, some elements markedly changed concentrations (Fe, Cu, Co, Cr, Ni, and Hg; Fig. 4), with similarities to the FE plant in 2022 samples. The precious elements, Ag and Au, are higher in FAL than FAS samples. In FAL samples, Ag and Au decrease over time, except for a concentration peak of Au in FC plant in 2020. Interestingly, the average content of I is always higher in FAS than in FAL (Fig. 4; Fig. S5 vs Fig. S6), likely because the Na-rich additive can retain I better than the Ca-rich one.

The temporal variation observed can be correlated to the different waste sorting, incineration technologies, and treatment performances that are expected to vary, according to the European Environmental Agency (EEA, 2016). CRM, such as Ti, Co, V, Ga, and REE, are primarily concentrated in the 2013 samples, and their concentration pattern decreases over time for both plants (Fig. S2). The 2013 samples data show outliers (e.g., Al, Fe, Cu, Zn, Ba, W, and PGE), which may be attributed to ageing reactions (Santos et al., 2013) and variations in the MSW input and combustion process. The 2013-sample data compared to the most recent likely suggest improvements in phase separation and waste recycling. The differences outlined might be influenced by quantity and quality of certain input MSW (i.e., household waste, medical waste, industrial waste, packaging materials, and electronic waste) and/or variation in flue gas treatment systems (e.g., Abanades et al., 2002). The production of e-waste, medical waste, equipment and sanitisation products increased during COVID-19 pandemic, possibly explaining elemental variations of, e.g., Hg, Pb, Cd, Cr, Ni, and I. In particular, during the COVID-19 pandemic, the use of single-use plastics likely containing some PTE for fire resistance or antibiotic activity/sterilisation has significantly increased, mainly due to the necessity of personal protective equipment such as masks, gloves, and other throwaway plastics, which are finally destined for MSW, especially as unsorted collection. Although all evidence indicates that incineration is a method capable of permanently eliminating plastic waste, some unburned material still exists, especially in BA, which may still contain a minimal content of (micro)plastics-related substances (Yang et al., 2021). Nonetheless, incineration has been identified as a critical and precautionary strategy for the safe management of MSW during pandemics, such as the COVID-19 pandemic. Alterations in both the quantity and composition of MSW streams, as well as an enhanced microplastics content during the COVID-19 pandemic, may have led to changes in the activity of radionuclides and elemental content. Thereby, the combustion of such contaminated waste increases the likelihood of emitting hazardous byproducts, which should be monitored in future studies to avoid potential human health issues.

Our results are similar to those of Zhao et al. (2021), reporting high levels of Zn and Cu in BA and FA detected during seasonal assessment, in particular in the warmer season when incineration procedures may vary. Zhao et al. (2021) reported high mean concentrations of Cd, Cr, Ni, and As in FA during seasonal fluctuations in MSWI plant in Beijing, China. Valentim et al. (2024) reported similar high values of Cu, Zn, Pb and As concentration in FA collected over six months from a MSWI plant in Portugal (Table S4). Although the decreasing REE trend, average ∑REE concentrations recorded in FA from Shanxi MSWI plant (Cui and Qin, 2023) are lower than ∑REE values presented here (Table S4). Fig. 4 and Figures S1, S2 and S3, show elemental concentrations in BA, FAL, and FAS between MSWI plants, year of sampling, and seasonality (winter/-summer). The results of the independent sample *t*-test conducted to different populations (BA, FAL, and FAS) for the assessment of statistical difference of elements within different plants (FE and FC) and seasons (winter and summer) are reported in Table S5 and Table S6, respectively. The BA and FA from FE and FC MSWI plants are not statistically (at 0.05 significance level) different (Table S5); BA and FA from winter and summer seasons are not statistically (at 0.05 significance level) different (Table S6). Significant *p*-values considering all sample categories pertain a handful of elements (Table S5: Ca, P, Se, and Tl; Table S6: Rb, W, and I). In BA, Mg, Sr, Au, and Re are statistically different considering the two populations of FE and FC. At the same time, elements such as Br, Co, Sb, V and PGE are statistically different seasonally. FAL (plant-wise: I, Pb, Sb, and Te; season-wise: Co, Mn, V, and REE) and FAS (plant-wise: Au, Cs, In, S, Ta and REE; season-wise: Au, Ge, Ta, REE and PGE) show another behaviour. Differences in non-significant p-values suggest that factors like waste heterogeneity can explain differences between plants or seasons.

### 3.3. Estimated annual flow

In accordance with the principle of mass conservation, our mass balance calculations based on chemical concentration data of MSWI samples assume that the inorganic elements of interest in the input waste are fully retained in BA, FAL, and FAS samples. This approach further assumes efficient flue gas cleaning and negligible elemental losses due to (diffuse or single-point) emissions. The contributions from Lime and Soda samples (i.e., additives) are subtracted from corresponding FA data to isolate the element concentrations originating from the waste itself (Table S7). The assumption that all Ca in FAL and all Na in FAS originated from the added Lime and Soda raw material, respectively, can be rejected because Na and Ca amounts are clearly sourced from both additives and input MSW.

The output flows of Fe and Al are very high on a yearly average, followed by K, Mg, P, Zn and Cu in both plants (Fig. 5 and Table S8), especially from BA streams. In BA, Fe and Al flow estimates are consistent to those reported by Mühl et al. (2024) from an Austrian MSWI plant and by Allegrini et al. (2014) from a Danish MSWI plant. Some CRM, such as Co, V, W, and Ga, show a significant flow (in terms of t $a^{-1}$ output), and seemingly constant all years of observation (Fig. 5). The average flow of Mg increases, while Ba, P, and Ti flows decrease over time. Although Mg is statistically different in BA from two MSWI plants (Table S5), Mg-rich MSW input can be increasing in the regional basin of collection. High P flow in both plants can be associated to MSW containing organic and inorganic compounds rich in phosphorus, and Ti could be derived from Ti-bearing minerals such as ilmenite and rutile in consumer products (Havukainen et al., 2016; Maldybayev et al., 2024). High amount of Co can be recovered from spent batteries (particularly lithium-ion batteries) and electronic waste (Granite et al., 2023). Industrial waste products, especially those resulting from the manufacturing of steel and other alloys, can contain V. Gallium is primarily found in electronic waste, particularly light-emitting diodes (LEDs) and semiconductors. A decrease overtime was observed for As, Cr, and Ni output flows, with Cr and Ni peaks in Dec-2021 samples (Fig. 5). These PTE found in MSWI residues are associated to electronic equipment, batteries, lamps, paints, leather, rubber, and others (Wei et al., 2022). In 2021, some PTE, especially Cr and Ni, flows are ten times higher than those reported earlier by Morf et al. (2013) in Switzerland and Funari et al. (2015).

The average flows of REE from FE and FC are similar (order of $10^2$ kg $a^{-1}$) for all years (Fig. 5), with the highest average flow observed for Ce, followed by Nd, La, Y, Sc, Gd, and Pr (Table S8). Average flows of PGE such as Pt, Os, and Pd are all years very low, ranging 0.02–0.60, 0.22–13.6, and 0.01–7.24 kg $a^{-1}$, respectively. These low flows of PGE

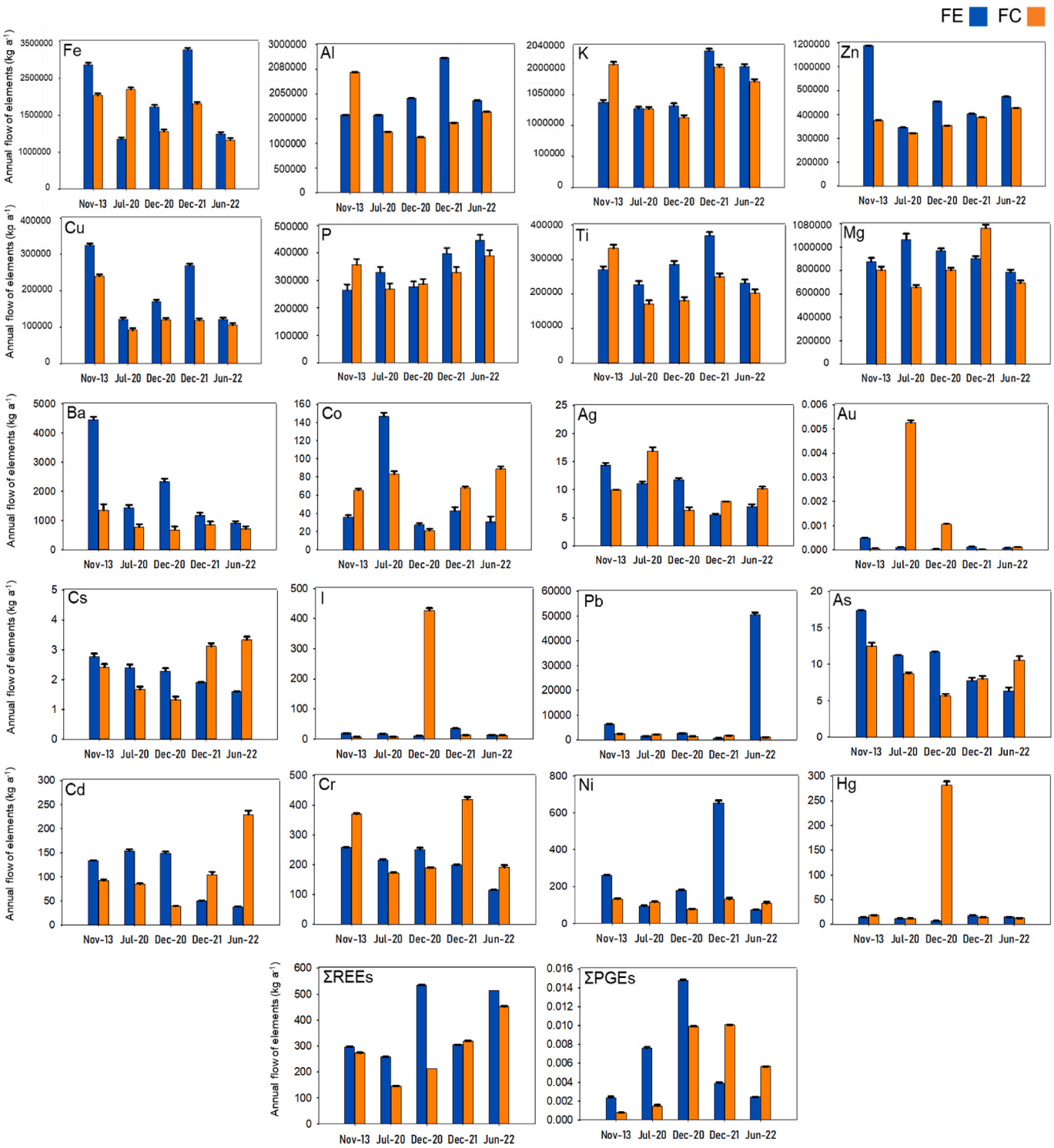


**Fig. 5.** Estimated annual flow of elements (kg $a^{-1}$) for all feeding input waste materials of FAL, FAS and BA from FE and FC in time series analysis. Results were calculated in (kg $a^{-1}$) on the basis of mass balance calculations (see section 2.6). Refer to Fig. 2 for the element selection.

are consistent to previous substance flow analysis of MSWI residues (e.g., Jackson et al., 2010; Allegrini et al., 2014; Funari et al., 2015). In both FE and FC, a flow of Ag and Au of about tens of kg $a^{-1}$ can reflect their presence in electronic scrap (Brandl et al., 2008). A previous study proposed that most Au elemental mass fraction of Swiss MSW is associated to WEEE (Müller et al., 2010). Therefore, some WEEE fractions ended up in MSW in FE and FC plants, likely due to the increasing use/wasting of electronics over time (from 2013 to 2022).

### 3.4. Activity concentrations of radionuclides

Results of radionuclides activity concentrations ($^{210}$Pb, $^{40}$K, $^{226}$Ra, $^{232}$Th, $^{137}$Cs, $^{241}$Am, $^{131}$I) in BA and FA (FAL, FAS) samples for 2013 and 2022 are presented in Fig. 6 and Table S9. Naturally occurring

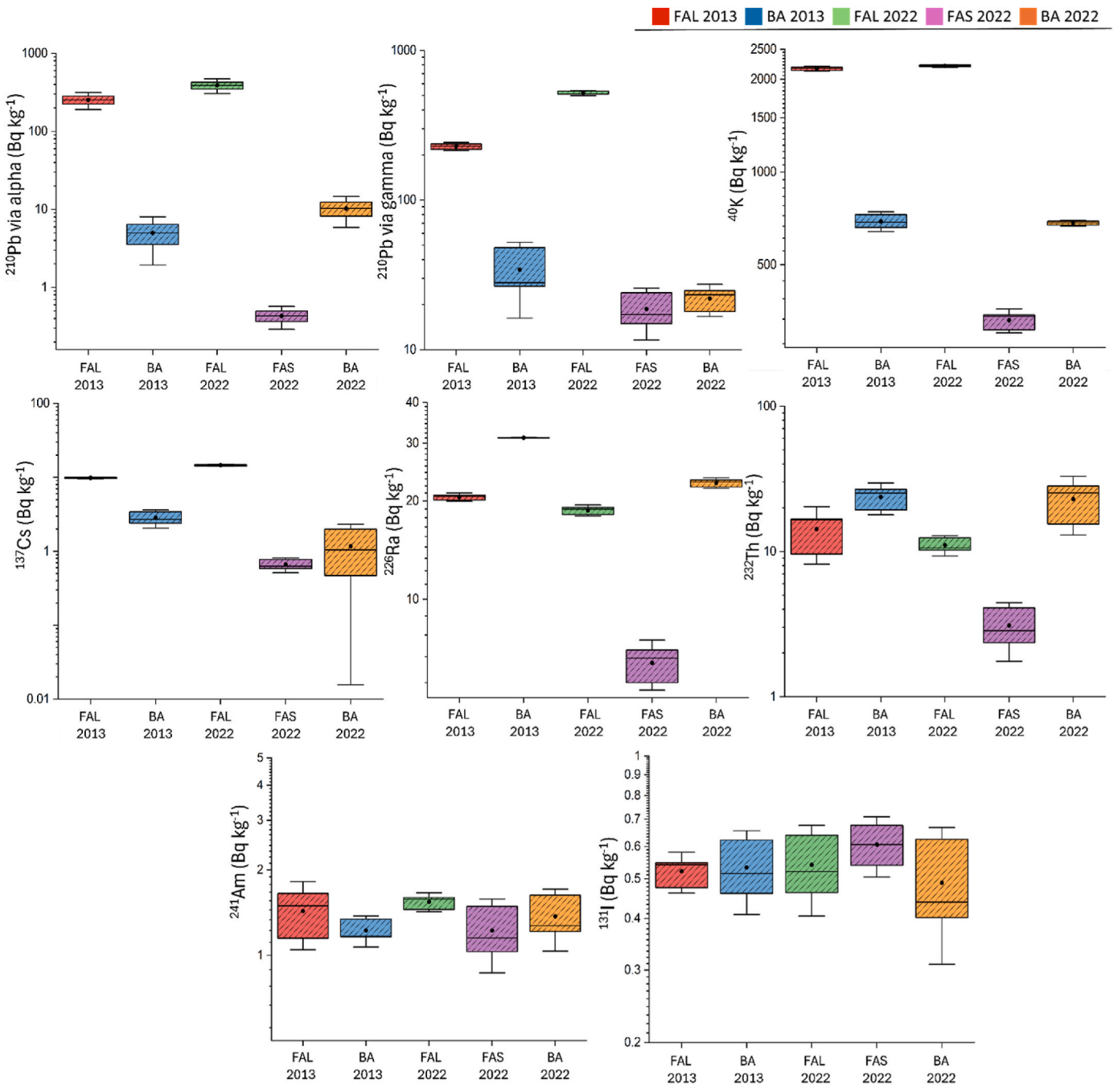


**Fig. 6.** Activity concentration (Bq kg$^{-1}$) of selected radionuclides in BA, FAL, and FAS from the FC plant, in 2013, and 2022.

radionuclides ($^{210}$Pb, $^{40}$K, $^{226}$Ra, and $^{232}$Th) are higher in FAL than FAS and BA, while the anthropogenic radionuclides ($^{137}$Cs, $^{241}$Am, and $^{131}$I) are comparatively low in all samples for all years (Fig. 6; Table S9). These radionuclides pose potential risks due to their radioactive decay and assessing their distribution in environmental matrices is crucial for radiation safety.

The activity of all radionuclides shows a similar behaviour for BA in 2013 and 2022. $^{40}$K is recorded with high activities, while $^{226}$Ra and $^{232}$Th are low in 2013 and 2022 (Fig. 6). High activities of $^{40}$K and moderate activities of $^{232}$Th are associated with inorganic materials in MSWI residues, while $^{238}$U-radioactive decay series like $^{226}$Ra is associated with organic material as MSW sent to MSWI plants (Papastefanou, 2010). $^{137}$Cs, $^{241}$Am, and $^{131}$I have low mean values (<3 Bq kg$^{-1}$). Results of $^{226}$Ra and $^{232}$Th in BA are comparable to those reported for BA from coal fired power plants in Turkey (Ozden et al., 2018). The activity of $^{40}$K, $^{226}$Ra, and $^{232}$Th is similar, $^{210}$Pb is higher, and $^{241}$Am is lower than that measured in BA and FA from nine MSWI plants in Finland (Kallio et al., 2023). Activity concentrations through alpha and gamma detectors of $^{210}$Pb in the 2013 FAL samples are lower than FAL samples of 2022 (Fig. 6 and Table S9). Alpha and gamma measurements on the same samples show slightly different results since the acid extraction used in the alpha measurement protocol is partial, while the gamma counting is performed on the bulk material. Despite this, alpha and gamma measurement results for both FAL 2013 and 2022 agree to the same order of magnitude, confirming the validity of the two analytical procedures for monitoring purposes. The highest activity of $^{40}$K was observed in FAL samples of 2013 and 2022 (Table S9). Activities of $^{226}$Ra are low and similar to those of $^{232}$Th (Fig. 6). The activities of $^{226}$Ra and

$^{232}$Th are lower in FAS than in FAL. High activity of $^{40}$K is recorded in FAS samples but seven times lower than that of FAL samples. Activity concentrations of $^{210}$Pb are also low but highest in FAL samples. In FAL and FAS, $^{137}$Cs, $^{241}$Am, and $^{131}$I activities are markedly low (<2 Bq kg$^{-1}$) and constant over time. Volatile radionuclides of Pb and Cs are generally lower in BA than FA, as previously observed between BA and FA from coal combustion (Sahu et al., 2014). High $^{210}$Pb can be originated from synthetic phosphor-gypsum and construction materials as cemetery wastes, while high $^{137}$Cs in 2013 might originate from bark wood, old leaves, birch and spruce mixed in MSW (Yoshida et al., 2011). Increased activities of $^{131}$I and $^{241}$Am are likely derived from smoke alarms in household wastes (Kallio et al., 2023). In conclusion, these nuclides can continuously end up in MSW and incineration facilities, but their abundance and activity levels are very low and pose no harm to humans. The overall health of the ecosystem should be assessed and monitored in future studies through multidisciplinary approaches.

### 3.4.1. *Radionuclides' enrichment factors and radiation hazard*

In BA, low EFs (<3) are for $^{210}$Pb and $^{232}$Th, $^{137}$Cs, and $^{131}$I, whereas a significant enrichment of $^{40}$K is estimated for 2013 and 2022 samples, with similar EFs of 247 and 244, respectively. EFs showed that radionuclides are enriched up to high levels in the FA, specifically FAL (Fig. 7a). In FAL, $^{137}$Cs, $^{232}$Th and $^{131}$I show low EFs (<10), and moderate EFs are for $^{210}$Pb (~100), while $^{40}$K has the highest EFs (>2600) for 2013 and 2022 samples. High $^{40}$K enrichment suggests that K volatilises and deposits on volatile ash particles (Knudsen et al., 2004), eventually depleting $^{40}$K contents in BA. The FAS category shows a high EF of 216 for $^{40}$K, while $^{210}$Pb displayed a much lower value (2), followed by $^{137}$Cs, $^{232}$Th and $^{131}$I (Fig. 7a).

The results of ACIs show that BA presented low values (<0.5) for both 2013 and 2022. The highest values of ACI are 0.86 ± 0.028 mSv y$^{-1}$ and 0.85 ± 0.005 mSv y$^{-1}$ for FAL samples of 2013 and 2022, respectively (Fig. 7b). A low value (0.14 ± 0.019 mSv y$^{-1}$) is estimated for FAS in 2022 (Fig. 7b). Similar ACIs (especially to FAL) were reported from thermoelectric power plants in Spain (Caño et al., 2023). All ACI values and their global average of 0.91 are found below the recommended permissible limit of 1 (European Commission, 1999). This means that activity concentrations from BA and FA fractions do not pose any potential radiological hazards to human health in the external environment.

### 3.4.2. *Total radionuclide emissions*

Total radionuclide emissions are estimated based on radioactivity levels measured in samples of the FC plant (FC estimation) (Fig. 7c). Moreover, a regional estimation could consider volumes of treated waste for 6 incinerators plants, i.e., available WtE facilities across the Emilia-Romagna region, Italy (Fig. 7d and Table S10). Total emissions of natural radionuclides in BA and FA (FAL and FAS) are substantially similar for 2013 and 2022. Highest emissions are observed for $^{40}$K, followed by $^{210}$Pb. Total annual emission of radionuclides from FAS is lower than FAL or BA emissions. In FAL, $^{226}$Ra shows moderate emissions, which increased by 80 %, on the regional scale, from 2013 to 2022 (Fig. 7c and d). Emissions of $^{210}$Pb and $^{40}$K are high, while $^{137}$Cs, $^{232}$Th, $^{131}$I and $^{241}$Am vary from low to moderate levels. This annual estimation revealed that the potential risk of radiological hazard is high for some nuclides. Hence, the assessment of radiological emissions from BA and

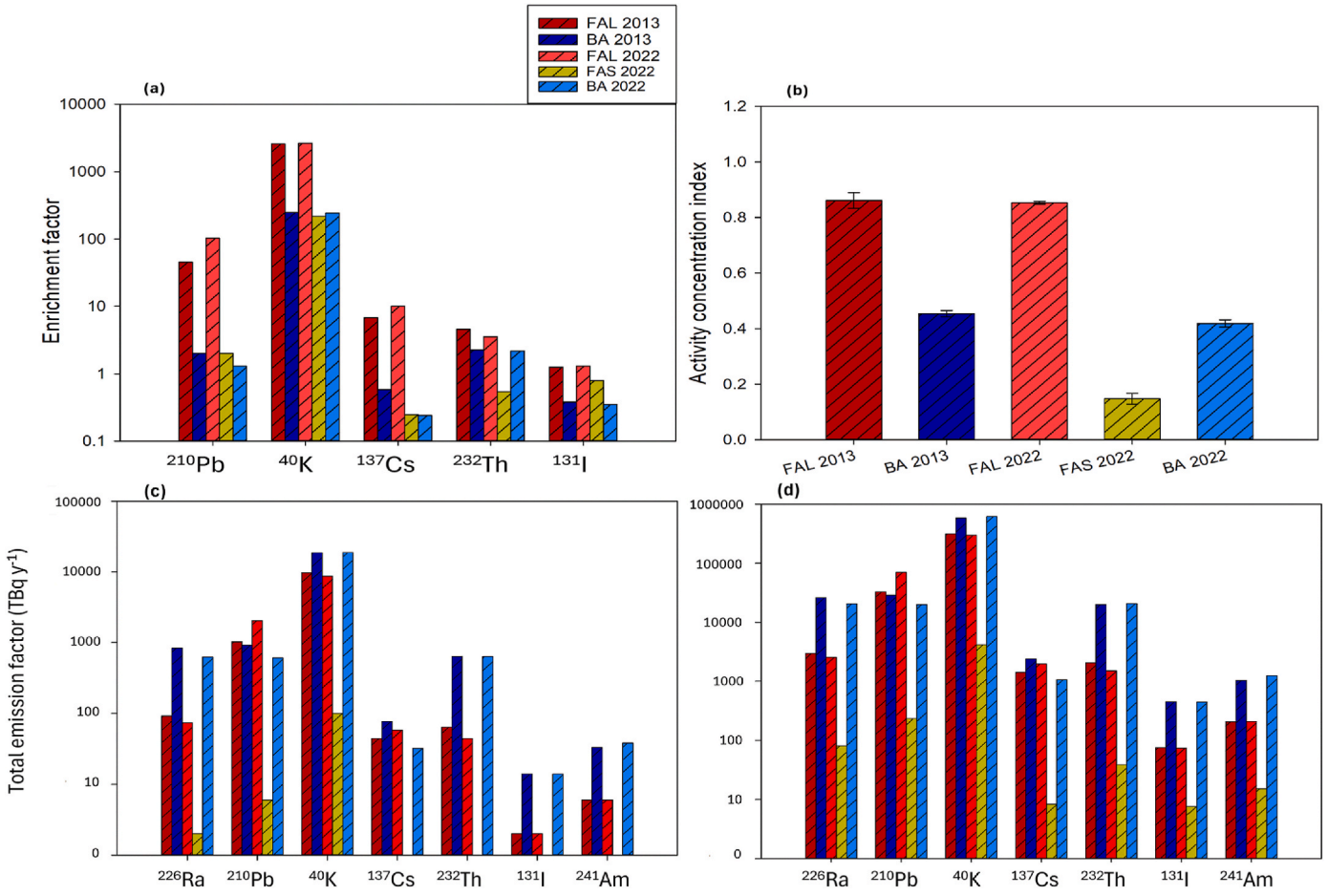


**Fig. 7.** (a) Enrichment factors (EFs) of selected radionuclides; (b) Activity concentration indexes (ACIs) in FAL, FAS, and BA from the FC plant, sampled in 2013 and 2022; (c) Total emission factor (TBq y$^{-1}$) of radionuclides of FC estimation; and (d) regional estimation of 6 incinerator plants of Emilia-Romagna region, Italy.

FA is crucial for assessing environmental impacts and help decision-makers.

## 4. Conclusion

This study presents a characterisation of Bottom (BA) and Fly Ash (FA) samples, including lime-doped, FAL, and soda-doped, FAS, taken in 2013, 2020, 2021 and 2022 from two incinerator plants (FE and FC) in Italy, detailing a selection of samples for their elemental abundance and radionuclide activity.

Elements like Fe, Al, Cu, Zn, P, Mg, Ti, Co, V, W, Ga, Ag, and REE (especially Ce) show high mean concentrations in BA, followed by FAL and FAS. These elements' abundance in solid residues is higher in 2013 than in 2020, 2021, and 2022, indicating a decrease in valuable elements from MSWI streams of substances. Heterogeneity in the chemical composition of MSW and related output flows of elements can complicate the recovery strategies. Understanding similarities and differences with other MSWI systems can prompt strategies for combined efforts to better utilise and manage MSWI residues. The substance flow analysis indicates significant elemental flows, including critical raw material, CRM, and potentially toxic elements, PTE. Remarkable flows of Fe, Al, Zn, Cu, Mg, Ti, Ag, and REE highlight the resource recovery potential of MSWI residues.

Time series analysis applied to MSWI residues can be a powerful tool for understanding how incineration waste feedstock has evolved for a given population, which can help define good practices in the waste management sector and subsequent urban mining. Declining trends for many elements over time likely suggest an improvement in sorting, regulations, and consumption patterns. Volatile elements like Zn, Pb, Cd, Ni, and Hg seem enriched in recent samples (i.e., after the COVID-19 pandemic). In all samples, major elements like Fe, Al, K, P, and Mg vary over time and can enrich seasonally (e.g., P in summer and Ni in winter), as well as REE fluctuate. After normalisation to chondrite reference values, REE patterns showed anomaly peaks for Ce, Pr, Nd, Gd, Tb, and Yb in most samples. In particular, high concentrations of Ag, Au, REE, and PGE possibly suggest incomplete separation of waste from electric and electronic equipment.

The activity of eight nuclides was assessed in samples from 2013 to 2022. Natural radionuclides (e.g., $^{40}K$, $^{210}Pb$) dominate over artificial ones, but Activity Concentration Index (ACI) values remain below safety thresholds, indicating no potential radiological hazards to humans in the external environment. However, enrichment factors (EF) suggest the accumulation of some radionuclides in FA over time, especially FAL.

A thorough assessment of elemental contents, resource flow, and emission factors of radionuclides in MSWI residues is crucial for informing life-cycle assessment inventories and policymaking. This study calls for new, multidisciplinary, and long-term assessments of MSWI systems.

## CRediT authorship contribution statement

**Junaid Ghani:** Writing – review & editing, Writing – original draft, Methodology. **Katerina Rodiouchkina:** Writing – review & editing, Supervision, Methodology, Formal analysis. **Ilia Rodushkin:** Writing – review & editing. **Enrico Dinelli:** Writing – review & editing, Supervision, Project administration, Methodology, Funding acquisition, Formal analysis. **Silvia Giuliani:** Writing – review & editing, Methodology. **Luca Giorgio Bellucci:** Writing – review & editing, Methodology. **Thomas Aiglsperger:** Writing – review & editing, Supervision. **Emma Engström:** Writing – review & editing. **Valerio Funari:** Writing – review & editing, Supervision, Project administration, Methodology, Formal analysis, Conceptualization.

## Environmental implication

European regulations classify MSWI residues as hazardous waste, particularly FA (Decision, 2000/532/EC). Additionally, the high flows of valuable elements make MSWI residues a potentially alternative resource for the circular economy. Minimising landfilling through appropriate treatments can also reduce the radiological hazard. The present study provides information that enables a comparative assessment of elemental contents and potential radiological impacts.

## Declaration of competing interest

The authors declare that they have no known competing financial interests or personal relationships that could have appeared to influence the work reported in this paper.

## Acknowledgements

The authors would like to express their appreciation to the Department of Biological, Geological and Environmental Sciences (BiGeA) of the University of Bologna that prompted this collaborative research through the project "*Sustainable Exploitation of Hidden Resources: approaches for Metal Recovery and Environmental Remediation*" in collaboration with National Research Council of Italy (CNR) - Marine science institute (ISMAR). The authors acknowledge the ICP-MS laboratory "Bruno Capaccioni" of BiGeA, University of Bologna, CNR Bologna Research Area with ISMAR infrastructures and laboratories (for sedimentology, geochemistry, and radiometry), Luleå University of Technology, and ALS Scandinavia AB, ALS Laboratory Group of Luleå, Sweden. We warmly thank the technical staff of HERAmbiente Incinerators for granting access to the facility and for their support in sampling. We also acknowledge that J.G. spent a three-month research visit at the Luleå University of Technology, where, thanks to a clean laboratory (Class 10,000, ALS Scandinavia AB laboratory) in Luleå, Sweden, solid sample digestion and ICP-SFMS analysis were performed. Finally, we warmly thank three anonymous reviewers for their constructive suggestions and the journal Editor for handling the manuscript. CNR provided financial support for this publication.

## Appendix A. Supplementary data

Supplementary data to this article can be found online at https://doi.org/10.1016/j.jenvman.2025.126977.

## Data availability

Data will be made available on request.

## References

Abanades, S., Flamant, G., Gauthier, D., 2002. Kinetics of heavy metal vaporization from model wastes in a fluidized bed. Environ. Sci. Technol. 36, 3879–3884. https://doi.org/10.1021/es020037e.

Ajorloo, M., Ghodrat, M., Scott, J., Strezov, V., 2022. Heavy metals removal/stabilization from municipal solid waste incineration fly ash: a review and recent trends. J. Mater. Cycles Waste Manag.t. 24, 1693–1717. https://doi.org/10.1007/s10163-022-01459-w.

Al-Ejji, M., Hassan, M.K., Youssef, K., Elmakaty, F., Mehanna, H., Sliem, M., Irshidat, M., 2023. Novel surface-treatment for bottom ash from municipal solid waste incineration to reduce the heavy metals leachability for a sustainable environment. J. Environ. Manag. 347, 119105. https://doi.org/10.1016/j.jenvman.2023.119105.

Allegrini, E., Maresca, A., Olsson, M.E., Holtze, M.S., Boldrin, A., Astrup, T.F., 2014. Quantification of the resource recovery potential of municipal solid waste incineration bottom ashes. Waste Manag. 34, 1627–1636. https://doi.org/10.1016/j.wasman.2014.05.003.

Axelsson, M.D., Rodushkin, I., Ingri, J., Öhlander, B., 2002. Multielemental analysis of Mn–Fe nodules by ICP-MS: optimisation of analytical method. Analyst 127, 76–82. https://doi.org/10.1039/B105706P.

Back, S., Sakanakura, H., 2021. Distribution of recoverable metal resources and harmful elements depending on particle size and density in municipal solid waste incineration bottom ash from dry discharge system. Waste Manag. 126, 652–663. https://doi.org/10.1016/j.wasman.2021.04.004.

Baxter, M., 1993. Environmental radioactivity: a perspective on industrial contributions. IAEA Bull. 35, 33–38.

Bellucci, L., Frignani, M., Cochran, J., Albertazzi, S., Zaggia, L., Cecconi, G., Hopkins, H., 2007. $^{210}$Pb and $^{137}$Cs as chronometers for salt marsh accretion in the Venice Lagoon–links to flooding frequency and climate change. J. Environ. Radioact. 97, 85–102. https://doi.org/10.1016/j.jenvrad.2007.03.005.

Brandl, H., Lehmann, S., Faramarzi, M.A., Martinelli, D., 2008. Biomobilization of silver, gold, and platinum from solid waste materials by HCN-forming microorganisms. Hydrometallurgy 94, 14–17. https://doi.org/10.1016/j.hydromet.2008.05.016.

Brunner, P., Rechberger, H., 2004. Practical Handbook of Material Flow Analysislewis Publishers. Boca Raton.

Bunge, R., 2015. Recovery of metals from waste incinerator bottom ash. In: Holm, O., Thome-Kozmiensky, E. (Eds.), Removal, Treatment and Utilisation of Waste Incineration Bottom Ash, pp. 63–143.

Caño, A., Suárez-Navarro, J.A., Puertas, F., Fernández-Jiménez, A., Alonso, M.d.M., 2023. New approach to determine the activity concentration index in cements, fly ashes, and slags on the basis of their chemical composition. Materials 16, 2677. https://doi.org/10.3390/ma16072677.

Casella, C., Vadivel, D., Dondi, D., 2024. The current situation of the legislative gap on microplastics (MPs) as new pollutants for the environment. Water Air Soil Pollut. 235 (12), 778. https://doi.org/10.1007/s11270-024-07589-1.

Chuchro, M., Jędrusiak, R., Bielowicz, B., 2025. Statistical analyses of precious metal contents in waste incineration bottom ashes. Sci. Rep. 15 (1), 8149. https://doi.org/10.1038/s41598-025-91855-7.

Cui, H., Qin, Q., 2023. Morphological distribution and phase composition of rare earth elements in waste incineration fly ash. Acadlore Trans. Geosci. 2 (3), 167–176. https://doi.org/10.56578/atg020304.

Dal Pozzo, A., Antonioni, G., Guglielmi, D., Stramigioli, C., Cozzani, V., 2016. Comparison of alternative flue gas dry treatment technologies in waste-to-energy processes. Waste Manag. 51, 81–90. https://doi.org/10.1016/j.wasman.2016.02.029.

Dou, X., Ren, F., Nguyen, M.Q., Ahamed, A., Yin, K., Chan, W.P., Chang, V.W.-C., 2017. Review of MSWI bottom ash utilization from perspectives of collective characterization, treatment and existing application. Renew. Sustain. Energy Rev. 79, 24–38. https://doi.org/10.1016/j.rser.2017.05.044.

European Environmental Agency (EEA), 2016. Research Institute on Sustainable Economic Growth. National Research Council of Italy. IRCrES/CNR (a partner in the ETC/WMGE).

European Society of Radiology (ESR), 2015. Summary of the European Directive 2013/59/Euratom: essentials for health professionals in radiology. Insight. Imag. 6, 411–417 [online].

European Commission (EC), 1999. Directorate-General for Environment, N.S., Protection. Radiological protection principles concerning the natural radioactivity of building materials. THE Office.

European Commission (EC), 2023. European Commission, Study on the Critical Raw Materials for the EU 2023 - Final Report.

European Union (EU), 2020. Critical Raw Materials Resilience: Charting a Path Towards Greater Security and Sustainability. Brussels, Germany: EESC.

Ebert, B.A., Steenari, B.-M., Geiker, M.R., Kirkelund, G.M., 2020. Screening of untreated municipal solid waste incineration fly ash for use in cement-based materials: chemical and physical properties. SN Appl. Sci. 2, 802. https://doi.org/10.1007/s42452-020-2613-7.

Ebert, B.A., 2021. Valorization of MSWI Fly Ash for Use in Cement-based Materials. Technical University of Denmark, Department of Civil Engineering.

Engström, E., Stenberg, A., Senioukh, S., Edelbro, R., Baxter, D.C., Rodushkin, I., 2004. Multi-elemental characterization of soft biological tissues by inductively coupled plasma–sector field mass spectrometry. Anal. Chim. Acta 521, 123–135. https://doi.org/10.1016/j.aca.2004.06.030.

Frandsen, F.J., Laursen, K., Arvelakis, S., 2004. Ash Chemistry in MSW Incineration Plants: Advanced Characterization and Thermodynamic Considerations. Final Technical Report in EFP Project, J. No. 1373/01-0029.

Funari, V., Braga, R., Bokhari, S.N.H., Dinelli, E., Meisel, T., 2015. Solid residues from Italian municipal solid waste incinerators: a source for “critical” raw materials. Waste Manage. (Tucson, Ariz.) 45, 206–216. https://doi.org/10.1016/j.wasman.2014.11.005.

Funari, V., Bokhari, S.N.H., Vigliotti, L., Meisel, T., Braga, R., 2016a. The rare earth elements in municipal solid waste incinerators ash and promising tools for their prospecting. J. Hazard. Mater. 301, 471–479. https://doi.org/10.1016/j.jhazmat.2015.09.015.

Funari, V., Meisel, T., Braga, R., 2016b. The potential impact of municipal solid waste incinerators ashes on the anthropogenic osmium budget. Sci. Total Environ. 541, 1549–1555. https://doi.org/10.1016/j.scitotenv.2015.10.014.

Funari, V., Mantovani, L., Vigliotti, L., Tribaudino, M., Dinelli, E., Braga, R., 2018. Superparamagnetic iron oxides nanoparticles from municipal solid waste incinerators. Sci. Total Environ. 621, 687–696. https://doi.org/10.1016/j.scitotenv.2017.11.289.

Funari, V., 2022. Sustainability assessment of bioleaching for mineral resource recovery from MSWI ashes. Circ. Econ. Sustain. 2, 419–445. https://doi.org/10.1016/B978-0-12-821664-4.00023-6.

Funari, V., Toller, S., Vitale, L., Santos, R.M., Gomes, H.I., 2023. Urban mining of municipal solid waste incineration (MSWI) residues with emphasis on bioleaching technologies: a critical review. Environ. Sci. Pol. 30, 59128–59150. https://doi.org/10.1007/s11356-023-26790-z.

Funari, V., Ghani, J., Mantovani, L., 2024. Chapter 27 - resource recovery from municipal solid waste incineration bottom ash resource recovery from bottom ashes. In: Wang, Lei, Tsang, Dan, Yan, Jianhua (Eds.), Treatment and Utilization of Combustion Residues. Elsevier, pp. 511–531. https://doi.org/10.1016/B978-0-443-21536-0.00011-3, 2024.

Ghani, J., Toller, S., Dinelli, E., Funari, V., 2023. Impact and recoverability of metals from waste: a case study on bottom ash from municipal solid waste incineration plants. Front. Environ. Sci. 11, 1252313. https://doi.org/10.3389/fenvs.2023.1252313.

Gökelma, M., Vallejo-Olivares, A., Tranell, G., 2021. Characteristic properties and recyclability of the aluminium fraction of MSWI bottom ash. Waste Manag. 130, 65–73. https://doi.org/10.1016/j.wasman.2021.05.012.

Granite, E.J., Bromhal, G., Wilcox, J., Alvin, M.A., 2023. Domestic wastes and byproducts: a resource for critical material supply chains. Bridge 53, 59–66.

Han, S., Ju, T., Meng, Y., Du, Y., Xiang, H., Aihemaiti, A., Jiang, J., 2021. Evaluation of various microwave-assisted acid digestion procedures for the determination of major and heavy metal elements in municipal solid waste incineration fly ash. J. Clean. Prod. 321, 128922. https://doi.org/10.1016/j.jclepro.2021.128922.

Havukainen, J., Nguyen, M.T., Hermann, L., Horttanainen, M., Mikkilä, M., Deviatkin, I., Linnanen, L., 2016. Potential of phosphorus recovery from sewage sludge and manure ash by thermochemical treatment. Waste Manag. 49, 221–229. https://doi.org/10.1016/j.wasman.2016.01.020.

Jackson, M.T., Prichard, H.M., Sampson, J., 2010. Platinum-group elements in sewage sludge and incinerator ash in the United Kingdom: assessment of PGE sources and mobility in cities. Sci. Total Environ. 408, 1276–1285. https://doi.org/10.1016/j.scitotenv.2009.09.014.

Janković, M.M., Todorović, D., Krneta-Nikolić, J.D., 2011. Analysis of natural radionuclides in coal, slag and ash in coal-fired power plants in Serbia. J. Min. Metall., Sect. B Metall. 47, 149–155. https://doi.org/10.2298/JMMB110208008J.

Jiao, F., Zhang, L., Dong, Z., Namioka, T., Yamada, N., Ninomiya, Y., 2016. Study on the species of heavy metals in MSW incineration fly ash and their leaching behavior. Fuel Process 152, 108–115. https://doi.org/10.1016/j.fuproc.2016.06.013.

Kallio, A., Virtanen, S., Leikoski, N., Iloniemi, E., Kämäräinen, M., Hildén, T., Mattila, A., 2023. Radioactivity of residues from waste incineration facilities in Finland. J. Radiol. Prot. 43, 021502. https://doi.org/10.1088/1361-6498/acc596.

Kasina, M., Jarosz, K., Stolarczyk, M., Göttlicher, J., Steininger, R., Michalik, M., 2023. Characteristic of phosphorus rich compounds in the incinerated sewage sludge ashes: a case for sustainable waste management. Sci. Rep. 13, 9137. https://doi.org/10.1038/s41598-023-36407-7.

Keith, S., Wohlers, D., Ingerman, L., 2019. Toxicological Profile for Thorium.

Kermani, B., Roubi, E.E., Selim, M., Al Bosaeedi, A., Maisonneuvem, G., 2007. Corrosion performance of commercially pure titanium exchanger tubes in acid gas removal units; operational experience. In: NACE CORROSION (NACE-07394). NACE.

King, A.H., Eggert, R.G., 2022. Critical materials for permanent magnets. Modern Permanent Magnets. Elsevier, pp. 343–370. https://doi.org/10.1016/B978-0-323-88658-1.00003-0.

Knudsen, J.N., Jensen, P.A., Dam-Johansen, K., 2004. Transformation and release to the gas phase of Cl, K, and S during combustion of annual biomass. Energy Fuel. 18, 1385–1399. https://doi.org/10.1021/ef049944q.

Kolawole, T.O., Olatunji, O.S., Ajibade, O.M., Oyelami, C.A., 2021. Sources and level of rare earth element contamination of atmospheric dust in Nigeria. J. Health Pollut. 11, 210611. https://doi.org/10.5696/2156-9614-11.30.210611.

Lemaignan, C., 2012. 2.07-Zirconium alloys: properties and characteristics. J. Nucl. Mater. 2, 217–232.

Lou, Y., Jiang, S., Du, B., Dai, X., Wang, T., Wang, J., Zhang, Y., 2023. Leaching morphology characteristics and environmental risk assessment of 13 hazardous trace elements from municipal solid waste incineration fly ash. Fuel 346, 128374. https://doi.org/10.1016/j.fuel.2023.128374.

Lu, N., Ran, X., Pan, Z., Korayem, A.H., 2022. Use of municipal solid waste incineration fly ash in geopolymer masonry mortar manufacturing. Materials 15, 8689. https://doi.org/10.3390/ma15238689.

Maldybayev, G., Korabayev, A., Sharipov, R., Al Azzam, K.M., Negim, E.-S., Baigenzhenov, O., Alimzhanova, A., Panigrahi, M., Shayakhmetova, R., 2024. Processing of titanium-containing ores for the production of titanium products: a comprehensive review. Heliyon 10 (3), e24966. https://doi.org/10.1016/j.heliyon.2024.e24966.

Mantovani, L., De Matteis, C., Tribaudino, M., Boschetti, T., Funari, V., Dinelli, E., Toller, S., Pelagatti, P., 2023. Grain size and mineralogical constraints on leaching in the bottom ashes from municipal solid waste incineration: a comparison of five plants in northern Italy. Front. Environ. Sci. 11, 1179272. https://doi.org/10.3389/fenvs.2023.1179272.

McDonough, W.F., Sun, S.S., 1995. The composition of the Earth. Chem. Geol. 120 (3–4), 223–253. https://doi.org/10.1016/0009-2541(94)00140-4.

Menéndez-García, L.A., García-Nieto, P.J., García-Gonzalo, E., Lasheras, F.S., 2024. Time series analysis for COMEX platinum spot price forecasting using SVM, MARS, MLP, VARMA and ARIMA models: a case study. Resour. Policy 95, 105148. https://doi.org/10.1016/j.resourpol.2024.105148.

Mitra, A., Sen, I.S., Walkner, C., Meisel, T.C., 2021. Simultaneous determination of platinum group elements and rhenium mass fractions in road dust samples using isotope dilution inductively coupled plasma-tandem mass spectrometry after cation exchange separation. Spectrochim. Acta Part B At. Spectrosc. 177, 106052. https://doi.org/10.1016/j.sab.2020.106052.

Morf, L.S., Gloor, R., Haag, O., Haupt, M., Skutan, S., Di Lorenzo, F., Boni, D., 2013. Precious metals and rare earth elements in municipal solid waste – sources and fate in a Swiss incineration plant. Waste Manage. (Tucson, Ariz.) 33 (3), 634–644. https://doi.org/10.1016/j.wasman.2012.09.010.

Mohamed, H., Pauzi, A., Ahmads, N., Karims, N., Wazirs, M., Bahri, C.Z., Idriss, M., 2023. Natural radioactivity analysis and radiological impact assessment from a coal power plant. Int. J. Radiat. Res. 21, 797–804. https://doi.org/10.61186/ijrr.21.4.797.

Mühl, J., Hofer, S., Blasenbauer, D., Lederer, J., 2024. Recovery of aluminum, magnetic ferrous metals and glass through enhanced industrial-scale treatment of different

MSWI bottom ashes. Waste Manag. 190, 557–568. https://doi.org/10.1016/j.wasman.2024.10.025.
Müller, E., Widmer, R., Im Auftrag des Bundesamtes für Umwelt, B., 2010. Materialflüsse der elektrischen und elektronischen Geräte in der Schweiz. Empa, Im Auftrag des Bundesamtes für Umwelt (BAFU).
Nedkvitne, E.N., Borgan, Ø., Eriksen, D.Ø., Rui, H., 2021. Variation in chemical composition of MSWI fly ash and dry scrubber residues. Waste Manag. 126, 623–631. https://doi.org/10.1016/j.wasman.2021.04.007.
Nguyen, T.T.T., Vuong, T.X., Pham, T.T.H., Hoang, Q.A., Tu, B.M., Nguyen, T.H., Nguyen, T.T.P., 2024. Insight into heavy metal chemical fractions in ash collected from municipal and industrial waste incinerators in northern Vietnam. RSC Adv. 14, 16486–16500. https://doi.org/10.1039/d4ra01465k.
Ozden, B., Guler, E., Vaasma, T., Horvath, M., Kiisk, M., Kovacs, T., 2018. Enrichment of naturally occurring radionuclides and trace elements in Yatagan and Yenikoy coal-fired thermal power plants, Turkey. J. Environ. Radioact. 188, 100–107. https://doi.org/10.1016/j.jenvrad.2017.09.016.
Ouyang, J., Song, L.J., Ma, L.L., Luo, M., Shao, Y., Dai, X.X., Yang, G.S., Yang, Y.G., Luo, M.Y., Xu, D.D., 2018. Temporal variations, sources and tracer significance of Polonium-210 in the metropolitan atmosphere of Beijing, China. Atmos. Environ. 193, 214–223. https://doi.org/10.1016/j.atmosenv.2018.09.005.
Papastefanou, C., 2010. Escaping radioactivity from coal-fired power plants (CPPs) due to coal burning and the associated hazards: a review. J. Environ. Radioact. 101, 191–200. https://doi.org/10.1016/j.jenvrad.2009.11.006.
Perry, A., Van Veen, K., 2024. Recovering rare Earth elements from E-Waste: potential impacts on NdFeB magnet supply chains and the environment. J. Int'l Com. Econ. 1.
Pontér, S., Sutliff-Johansson, S., Engström, E., Widerlund, A., Mäki, A., Rodushkina, K., Paulukat, C., Rodushkin, I., 2021. Evaluation of a multi-isotope approach as a complement to concentration data within environmental forensics. Minerals 11, 37. https://doi.org/10.3390/min11010037.
Prata, J.C., Silva, A.L., Walker, T.R., Duarte, A.C., Rocha-Santos, T., 2020. COVID-19 pandemic repercussions on the use and management of plastics. Environ. Sci. Technol. 54, 7760–7765. https://doi.org/10.1021/acs.est.0c02178.
Quina, M.J., Bontempi, E., Bogush, A., Schlumberger, S., Weibel, G., Braga, R., Funari, V., Hyks, J., Rasmussen, E., Lederer, J., 2018. Technologies for the management of MSW incineration ashes from gas cleaning: new perspectives on recovery of secondary raw materials and circular economy. Sci. Total Environ. 635, 526–542. https://doi.org/10.1016/j.scitotenv.2018.04.150.
Rissler, J., Klementiev, K., Dahl, J., Steenari, B.-M., Edo, M., 2020. Identification and quantification of chemical forms of Cu and Zn in MSWI ashes using XANES. Energy Fuel. 34, 14505–14514. https://doi.org/10.1021/acs.energyfuels.0c02226.
Rodushkin, I., Engström, E., Baxter, D.C., 2010. Sources of contamination and remedial strategies in the multi-elemental trace analysis laboratory. Anal. Bioanal. Chem. 396, 365–377. https://doi.org/10.1007/s00216-009-3087-z.
Rodushkin, I., Nordlund, P., Engström, E., Baxter, D.C., 2005. Improved multi-elemental analyses by inductively coupled plasma-sector field mass spectrometry through methane addition to the plasma. J. Anal. At. Spectrom. 20, 1250–1255. https://doi.org/10.1039/b507886e.
Rodushkin, I., Paulukat, C., Pontér, S., Engström, E., Baxter, D.C., Sörlin, D., Pallavicini, N., Rodushkina, K., 2018. Application of double-focusing sector field ICP-MS for determination of ultratrace constituents in samples characterized by complex composition of the matrix. Sci. Total Environ. 622, 203–213. https://doi.org/10.1016/j.scitotenv.2017.11.288.
Rogowska, J., Olkowska, E., Ratajczyk, W., Wolska, L., 2018. Gadolinium as a new emerging contaminant of aquatic environments. Environ. Toxicol. Chem. 37, 1523–1534. https://doi.org/10.1002/etc.4116.
Romano, P., Birloaga, I., Vegliò, F., 2023. Recovery of platinum and palladium from spent automotive catalysts: study of a new leaching System using a complete factorial design. Minerals 13, 479. https://doi.org/10.3390/min13040479.
Rudnick, R., Gao, S., 2014. In: Turekian, K.K., Holland, H.D. (Eds.), Composition of the Continental Crust. From: Treatise on Geochemistry, second ed. Elsevier Inc., New York, NY, pp. 1–51. https://doi.org/10.1016/B0-08-043751-6/03016-4. Chap. 2, vol. 4.
Sahu, S., Ohara, T., Beig, G., 2017. The role of coal technology in redefining India's climate change agents and other pollutants. Environ. Res. Lett. 12, 105006. https://doi.org/10.1088/1748-9326/aa814a.
Sahu, S., Tiwari, M., Bhangare, R., Pandit, G., 2014. Enrichment and particle size dependence of polonium and other naturally occurring radionuclides in coal ash. J. Environ. Radioact. 138, 421–426. https://doi.org/10.1016/j.jenvrad.2014.04.010.
Santos, R.M., Mertens, G., Salman, M., Cizer, Ö., Van Gerven, T., 2013. Comparative study of ageing, heat treatment and accelerated carbonation for stabilization of municipal solid waste incineration bottom ash in view of reducing regulated heavy metal/metalloid leaching. J. Environ. Manag. 128, 807–821. https://doi.org/10.1016/j.jenvman.2013.06.033.
Smołka-Danielowska, D., Kądziołka-Gaweł, M., Krzykawski, T., 2019. Chemical and mineral composition of furnace slags produced in the combustion process of hard coal. Int. J. Environ. Sci. Technol. 16, 5387–5396. https://doi.org/10.1007/s13762-018-2122-z.
Świetlik, R., Trojanowska, M., Karbowska, B., Zembrzuski, W., 2016. Speciation and mobility of volatile heavy metals (Cd, Pb, and Tl) in fly ashes. Environ. Monit. Assess. 188, 1–11.
Tang, P., Florea, M., Spiesz, P., Brouwers, H., 2015. Characteristics and application potential of municipal solid waste incineration (MSWI) bottom ashes from two waste-to-energy plants. Constr. Build. Mater. 83, 77–94. https://doi.org/10.1016/j.conbuildmat.2015.02.033.
Vainikka, P., Hupa, M., 2012. Review on bromine in solid fuels – part 2: anthropogenic occurrence. Fuel 94, 34–51. https://doi.org/10.1016/j.fuel.2011.11.021.
Valentim, B., Guedes, A., Kuźniarska-Biernacka, I., Dias, J., Predeanu, G., 2024. Variation in the composition of municipal solid waste incineration ash. Minerals 14 (11), 1146. https://doi.org/10.3390/min14111146.
Wang, P., Hu, Y., Cheng, H., 2019. Municipal solid waste (MSW) incineration fly ash as an important source of heavy metal pollution in China. Environ. Pollut. 252, 461–475. https://doi.org/10.1016/j.envpol.2019.04.082.
Wei, Y., Shimaoka, T., Saffarzadeh, A., Takahashi, F., 2011. Mineralogical characterization of municipal solid waste incineration bottom ash with an emphasis on heavy metal-bearing phases. J. Hazard. Mater. 187, 534–543. https://doi.org/10.1016/j.jhazmat.2011.01.070.
Wei, J., Li, H., Liu, J., 2022. Heavy metal pollution in the soil around municipal solid waste incinerators and its health risks in China. Environ. Res. 203, 111871. https://doi.org/10.1016/j.envres.2021.111871.
Wielinski, J., Gogos, A., Voegelin, A., Müller, C.R., Morgenroth, E., Kaegi, R., 2021. Release of gold (Au), silver (Ag) and cerium dioxide ($CeO_2$) nanoparticles from sewage sludge incineration ash. Environ. Sci. Nano 8 (11), 3220–3232. https://doi.org/10.1039/D1EN00497B.
Weibel, G., Eggenberger, U., Kulik, D.A., Hummel, W., Schlumberger, S., Klink, W., Fisch, M., Mäder, U.K., 2018. Extraction of heavy metals from MSWI fly ash using hydrochloric acid and sodium chloride solution. Waste Manag. 76, 457–471. https://doi.org/10.1016/j.wasman.2018.03.022.
Witard, O.C., Bath, S.C., Dineva, M., Sellem, L., Mulet-Cabero, A.I., van Dongen, L.H., Zheng, J.S., Valenzuela, C., Smeuninx, B., 2022. Dairy as a source of iodine and protein in the UK: implications for human health across the life course, and future Policy and research. Front. Nutr. 9, 800559. https://doi.org/10.3389/fnut.2022.800559.
Xiang, J., Qiu, J., Li, Z., Chen, J., Song, Y., 2022. Eco-friendly treatment for MSWI bottom ash applied to supplementary cementing: mechanical properties and heavy metal leaching concentration evaluation. Constr. Build. Mater. 327, 127012. https://doi.org/10.1016/j.conbuildmat.2022.127012.
Yang, Z., Lü, F., Zhang, H., Wang, W., Shao, L., Ye, J., He, P., 2021. Is incineration the terminator of plastics and microplastics? J. Hazard. Mater. 401, 123429. https://doi.org/10.1016/j.jhazmat.2020.123429.
Yao, J., Li, W.-B., Kong, Q.-N., Wu, Y.-Y., He, R., Shen, D.-S., 2010. Content, mobility and transfer behavior of heavy metals in MSWI bottom ash in Zhejiang Province, China. Fuel 89, 616–622. https://doi.org/10.1016/j.fuel.2009.06.016.
Yao, J., Qiu, Z., Kong, Q., Chen, L., Zhu, H., Long, Y., Shen, D., 2017. Migration of Cu, Zn and Cr through municipal solid waste incinerator bottom ash layer in the simulated landfill. Ecol. Eng. 102, 577–582. https://doi.org/10.1016/j.ecoleng.2017.02.063.
Yoshida, S., Watanabe, M., Suzuki, A., 2011. Distribution of radiocesium and stable elements within a pine tree. Radiat. Protect. Dosim. 146, 326–329. https://doi.org/10.1093/rpd/ncr181.
Zambon, A., Malavasi, G., Pallini, A., Fraulini, F., Lusvardi, G., 2021. Cerium containing bioactive glasses: a review. ACS Biomater. Sci. Eng. 7, 4388–4401. https://doi.org/10.1021/acsbiomaterials.1c00414.
Zhao, H., Tian, Y., Wang, R., Wang, R., Zeng, X., Yang, F., Wang, Z., Chen, M., Shu, J., 2021. Seasonal variation of the mobility and toxicity of metals in Beijing's municipal solid waste incineration fly ash. Sustainability 13, 6532. https://doi.org/10.3390/su13126532.
Zhao, L., Zhang, F.-S., Zhang, J., 2008. Chemical properties of rare earth elements in typical medical waste incinerator ashes in China. J. Hazard. Mater. 158, 465–470. https://doi.org/10.1016/j.jhazmat.2008.01.091.